PETROLOGY AND MASS-BALANCE CONSTRAINTS
ON THE ORIGIN OF QUARTZ-AUGEN SCHIST ASSOCIATED
WITH THE BRUNSWICK MASSIVE SULFIDE DEPOSITS,
BATHURST, NEW BRUNSWICK[1]

DAVID R. LENTZ

Geological Survey of Canada, P.O. Box 50, Bathurst, New Brunswick E2A 3Z1

WAYNE D. GOODFELLOW

Geological Survey of Canada, 601 Booth Street, Ottawa, Ontario K1A 0E8

ABSTRACT

Coarse-grained quartz–alkali feldspar crystal-rich tuff (QFAS) represents the least-altered host rock in the stratigraphic footwall volcaniclastic sequence at the Brunswick No. 12 massive sulfide deposit. Toward the sulfide deposit, the coarse-grained alkali feldspar phenoclasts exhibit variable degrees of pseudomorphic replacement by secondary quartz, albite, phengitic sericite, and Mg-rich chlorite to form milky quartz-rich augen. The proportion of albite decreases with increasing quartz and mica in pseudomorphs in the quartz-augen schist (QAS). The preservation of pseudomorph morphology in low-strain domains suggests that the pseudomorphs predate deformation and are the result of hydrothermal alteration. The mica compositions reflect the major-element changes resulting from increased alteration toward the ore zone. For example, the increase in Fe/(Fe+Mg) of chlorite, phengite, and whole rock from the less-altered rocks (0.30, 0.25, 0.70, respectively) to the most-altered rocks along the sample profile (0.75, 0.70, 0.90, respectively) reflects the increasing abundance of Fe and Fe-rich chlorite associated with the proximal alteration facies. Based on mass-balance calculations considering Al as least mobile, the weakly altered crystal-rich tuff (Q[F]AS) is enriched, relative to the least-altered crystal-rich tuff (QFAS), in Na, Fe, Mn, S, CO_2, and base metals, and has variable Mg and Ca contents. The moderately altered crystal-rich tuff (QAS) is enriched, with respect to the QFAS, in Fe, Mn, S, CO_2, and base metals, and depleted in Na, K, Ca, Ba, Rb, and Sr. SiO_2 is relatively unchanged. There has been 10 to 30% mass addition in the QAS relative to the QFAS. These alteration effects are more pronounced in the footwall tuffaceous sedimentary rocks just above the QAS contact, possibly because they are more reactive than the QFAS. The hydrolysis of primary and secondary feldspar to phengitic mica and Mg-rich chlorite is probably related to heated seawater alteration of the pyroclastic package on the margins of the discharging hydrothermal system. This peripheral assemblage is in turn replaced by Fe-rich chlorite and white mica toward the more highly altered QAS and footwall sedimentary rocks beneath the massive sulfide, which is indicative of moderately acidic and high $a\mathrm{Fe}^{2+}/a\mathrm{Mg}^{2+}$ conditions during hydrothermal alteration.

Keywords: footwall alteration, hydrothermal vent, feeder zone, quartz-augen schist, quartz-eye schist, Brunswick Mines, Bathurst, New Brunswick.

SOMMAIRE

Les tufs riches en cristaux grossiers de quartz et de feldspath alcalin représentent les roches hôtes les moins altérées de la séquence volcaniclastique stratigraphiquement en dessous du gîte à sulfures massifs de Brunswick No. 12, près de Bathurst, au Nouveau-Brunswick. Près de l'amas de sulfures, les phénocristaux grossiers de feldspath alcalin témoignent d'un remplacement plus ou moins avancé par quartz secondaire, albite, séricite phengitique et chlorite magnésienne, pour produire des augen riches en quartz laiteux. La proportion d'albite diminue à mesure qu'augmente la proportion de quartz et de mica dans les schistes à augen de quartz. La conservation de la morphologie du produit pseudomorphique dans les domaines faiblement déformés fait penser que la pseudomorphose a précédé la déformation, et résulterait d'une altération hydrothermale. La composition du mica illustre les changements en termes des éléments majeurs, de plus en plus importants près de la zone minéralisée. Par exemple, l'augmentation en Fe/(Fe + Mg) dans la chlorite, la phengite, et les roches totales, à partir des roches les moins altérées (0.30, 0.25 et 0.70, respectivement) vers les roches plus fortement altérées le long du même profil (0.75, 0.70 et 0.90, respectivement) témoigne de l'importance accrue du fer et d'une chlorite ferrifère en association avec le facies proximal de l'altération. A la lumière des calculs des bilans de masse, en considérant Al comme le moins mobile des éléments, les tufs à

cristaux qui sont faiblement altérés sont enrichis en Na, Fe, Mn, S, CO_2 et métaux de base par rapport aux roches les moins altérées, tandis que leurs teneurs en Mg et Ca sont variables. Les tufs à cristaux à degré d'altération moyen sont enrichis en Fe, Mn, S, CO_2 et métaux de base, et appauvris en Na, K, Ca, Ba, Rb, et Sr par rapport aux mêmes roches-témoins. SiO_2 demeure relativement constant. Il y a eu addition d'environ 10 à 30% de masse dans les roches les plus altérées. Ces effets sont plus prononcés dans les sédiments volcanogéniques de la paroi inférieure du gisement, possiblement à cause de leur plus grande réactivité. L'hydrolyse des feldspaths primaire et secondaire pour donner un mica phengitique et une chlorite magnésienne serait liée à l'altération de l'amas pyroclastique due à la circulation de l'eau de mer chauffée, dans les parties périphériques d'un système d'évents hydrothermaux. L'assemblage distal est ensuite remplacé par un assemblage à chlorite ferrifère + mica blanc dans la direction des roches plus fortement altérées sans feldspath et des roches métasédimentaires situées en dessous des sulfures massifs, ce qui indiquerait l'implication d'une phase fluide légèrement acide et à rapport $a\text{Fe}^{2+}/a\text{Mg}^{2+}$ élevé au cours de l'altération hydrothermale.

(Traduit par la Rédaction)

Mots-clés: altération de la paroi inférieure, évent hydrothermal, filon nourricier, schiste à augen de quartz, mines Brunswick, Bathurst, Nouveau-Brunswick.

INTRODUCTION

It has been known for some time that there is a common association between the occurrence of quartz-porphyroidal rocks and massive sulfide deposits in felsic volcanic sequences. The felsic pyroclastic rocks occurring stratigraphically beneath the "Brunswick horizon" massive sulfides and laterally equivalent Algoma-type iron formation were, for the most part, originally crystal-rich tuffs with quartz and feldspar phenoclasts and possibly porphyritic intrusions that were deformed and metamorphosed into quartz–feldspar augen schists (QFAS) (Loudon 1960, Lentz & Goodfellow 1992a; Fig. 1). There has been some controversy, however, over the origin of the quartz augen and their metallogenic significance primarily on the basis of textural evidence from numerous deposits, including those in the Bathurst Mining Camp, where these rocks are known as quartz-augen schists (QAS) or quartz-eye schists (QES). Hypotheses for the origin of quartz–augen-bearing rocks include porphyroblastic growth of quartz in siliceous rocks (Hopwood 1976, 1977), volcanic quartz (Vernon & Flood 1977, Vernon 1986), near-surface weathering of epiclastic feldspar (McCutcheon 1990, 1992), and hydrolysis of feldspar within the vent complex of a massive sulfide deposit (Goodfellow 1975a, b, Juras 1981, Nelson 1983, Luff *et al.* 1992). Within the hanging-wall sequence at the Brunswick No. 12 deposit, the absence of feldspar in the fine-grained, feldspar-phyric rhyolitic tuffs and tuffaceous sedimentary rocks also is peculiar. Interestingly, at the Heath Steele ACD and B deposits, a narrow zone of sericitization of feldspar occurs within the crystal-rich tuffs of the stratigraphic hanging-wall (Wahl 1978).

This paper describes textural and mineralogical evidence and mass-balance constraints on the transformation of QFAS to QAS in the vicinity of the Brunswick No. 12 deposit. In order to characterize the QFAS–QAS transition petrographically and geochemically as the ore zone is approached, two sections on the 850-and 750-meter levels (Figs. 2A, B) were selected from the Brunswick No. 12 deposit. Because these sections span only the margin of the feeder zone, the mineralogy and geochemistry have allowed us to quantify fluid–rock reactions along the margin of what was the hydrothermal vent complex.

This work constitutes a part of a Canada – New Brunswick Agreement on Mineral Development (NB–CAMD 1990–1995) project, the objective of which is to characterize the exhalative environment and hydrothermal alteration associated with the Brunswick massive sulfide deposits.

GEOLOGICAL SETTING

The rocks of the Bathurst Mining Camp in northeastern New Brunswick comprise a Cambro-Ordovician sequence of sedimentary and bimodal volcanic rocks, which was intruded by mafic and felsic plutons (Skinner 1974). This assemblage was subsequently intensely deformed and metamorphosed during Late Ordovician (Ashgillian) to Devonian time (van Staal & Fyffe 1991, van Staal *et al.* 1992). In the mine area, the sequence consists of intercalated quartz wacke and carbonaceous pelite of the Patrick Brook Formation (Miramichi–Tetagouche Group, Fig. 1) and is conformably overlain by rocks of the Tetagouche Group. The Tetagouche Group has been subdivided from the base upward into: (1) volcanic, volcaniclastic, and sedimentary rocks of the Nepisiguit Falls Formation (NF, Fig. 1), (2) dominantly rhyolite and hyalotuff sequence known as the Flat Landing Brook Formation (FLB, Figs. 1, 2), and (3) an upper sequence composed of red to black siltstones, mudstones, and chert intercalated with transitional, tholeiitic to alkaline, mafic volcanic rocks of the Boucher Brook Formation (BB, Figs. 1, 2; van Staal & Fyffe 1991, van Staal *et al.* 1992).

The Brunswick massive sulfide deposits and associated iron formation occur in the upper part of the NF Formation. The sulfide deposits are overlain by
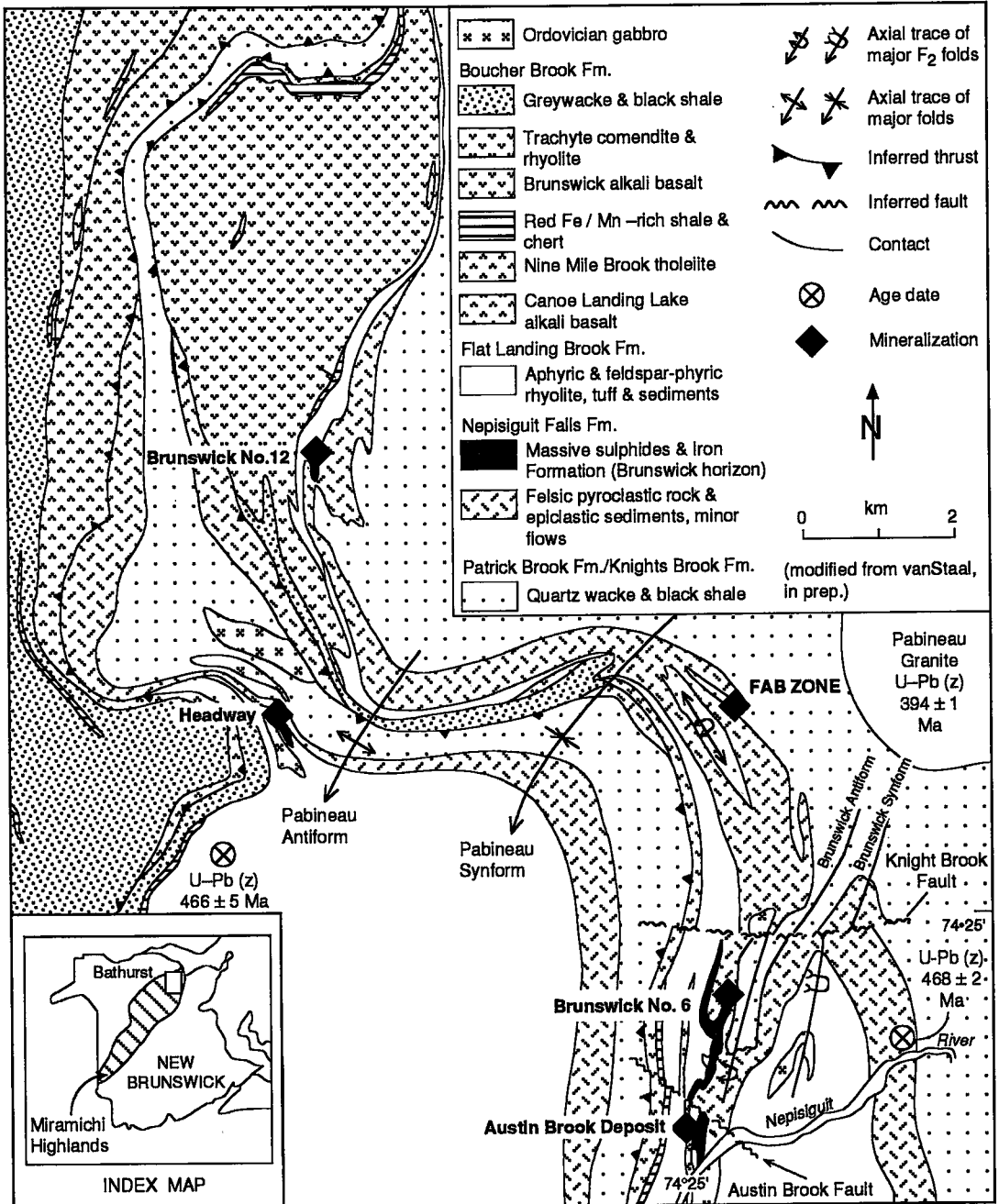
FIG. 1. Geological map of the Brunswick No. 6 and 12 areas, based on recent geological mapping of the area (modified after van Staal 1992).
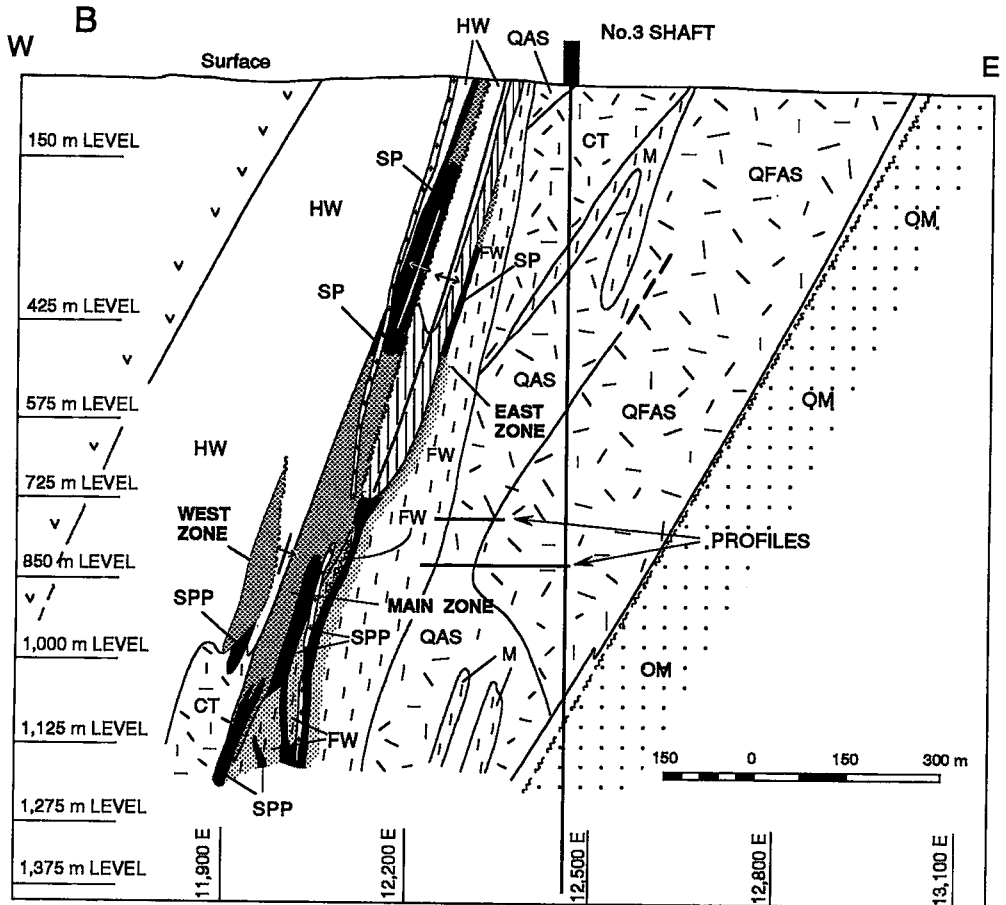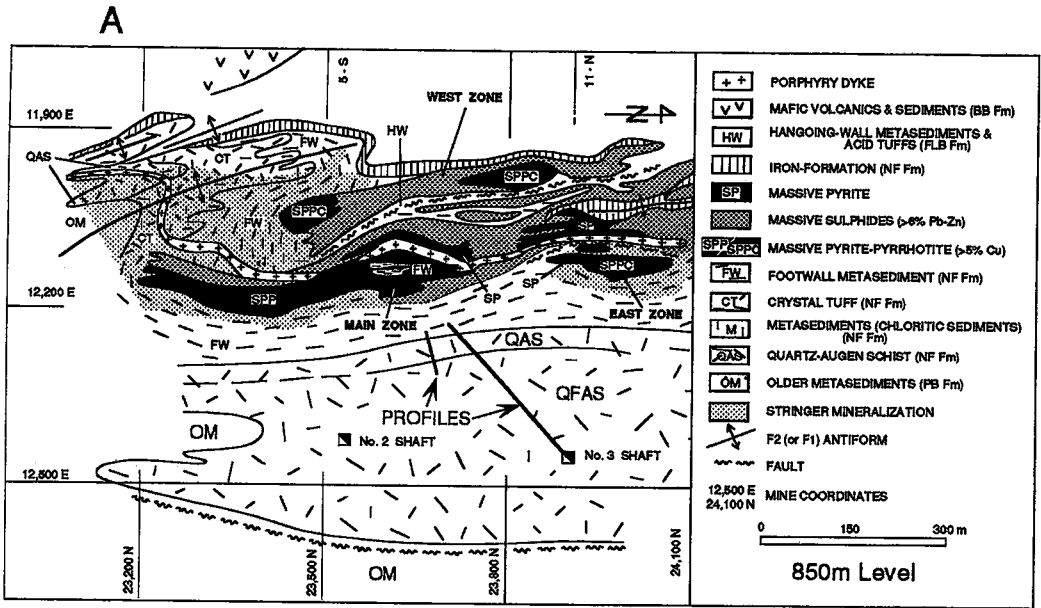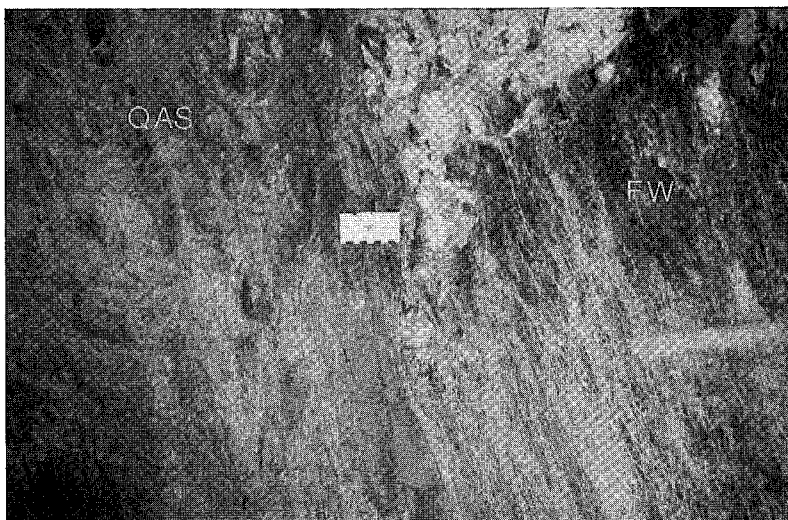
FIG. 3. Photograph of sheared contact with late quartz veins between the quartz-augen schist (QAS) and the footwall sedimentary rocks (FW) at sample location 006 (QAS) and 005A and B (FW).

rhyolitic volcanic rocks and associated sedimentary rocks of the FLB Formation. The upper part of the FLB Formation coincides with the transition from felsic to mafic volcanism within the back-arc rift (van Staal 1987, Fyffe & Swinden 1991).

At least five generations of folds have been identified in the Bathurst Mining Camp (van Staal 1985, 1987) The S_1 foliation is particularly well developed and is commonly transposed parallel to bedding. F_1 folds and S_1 foliations are associated with early thrust-faults and accompanying zones of high strain. F_2 folds are tight to isoclinal, with a strongly developed S_2 fabric. In the Brunswick Mines area, the F_2 axial trace is steeply dipping with moderate to shallow, doubly plunging axes. The interference between the F_2 folds and large northeast-trending F_5 folds (previously F_3 folds) is responsible for the geometric distribution of map units (van Staal & Williams 1984, van Staal 1987). Around the Brunswick No. 12 deposit, the rocks have undergone upper-greenschist-grade regional metamorphic conditions (M_1 and M_2), with temperatures on the order of 400°C estimated from various geothermometers (van Staal 1985, Lentz & Goodfellow 1993a) and the first appearance of biotite.

Pressures were on the order of 400 to 600 MPa (4 to 6 kbar) based on a petrogenetic grid and sphalerite geobarometry (van Staal 1985, Lentz & Goodfellow 1993a), and locally up to at least 700 MPa (7 kbar) within blueschists along a D_1 thrust zone between the Tetagouche Group and the Fournier Group to the northwest of the Brunswick No. 12 deposit (van Staal et al. 1990).

FOOTWALL LITHOTYPES

The Brunswick No. 6 and 12 massive sulfide deposits are hosted by volcaniclastic mudstones that are underlain by fine- to coarse-grained, crystal-rich tuffs (tufflavas), porphyritic intrusions and reworked pyroclastic and volcaniclastic rocks of the NF Formation (Figs. 2, 3, 4). In the vicinity of Brunswick No. 12 deposit, tight F_1 and F_2 folds are responsible for the development of the weak to strong S_1 and S_2 fabrics, which have transformed the crystal-rich tuffs and sedimentary rocks into augen schists. The distribution of the crystals, fragments, and matrix (originally glass) in these rocks has been variably modified by sedimentary reworking.

FIG. 2. A) Geological plan of the 850 m level, and B) geological section through the No. 3 shaft (11 north) at the Brunswick No. 12 deposit (modified after Luff et al. 1992), illustrating the distribution of QAS and QFAS on this level and the two profiles sampled for this study.
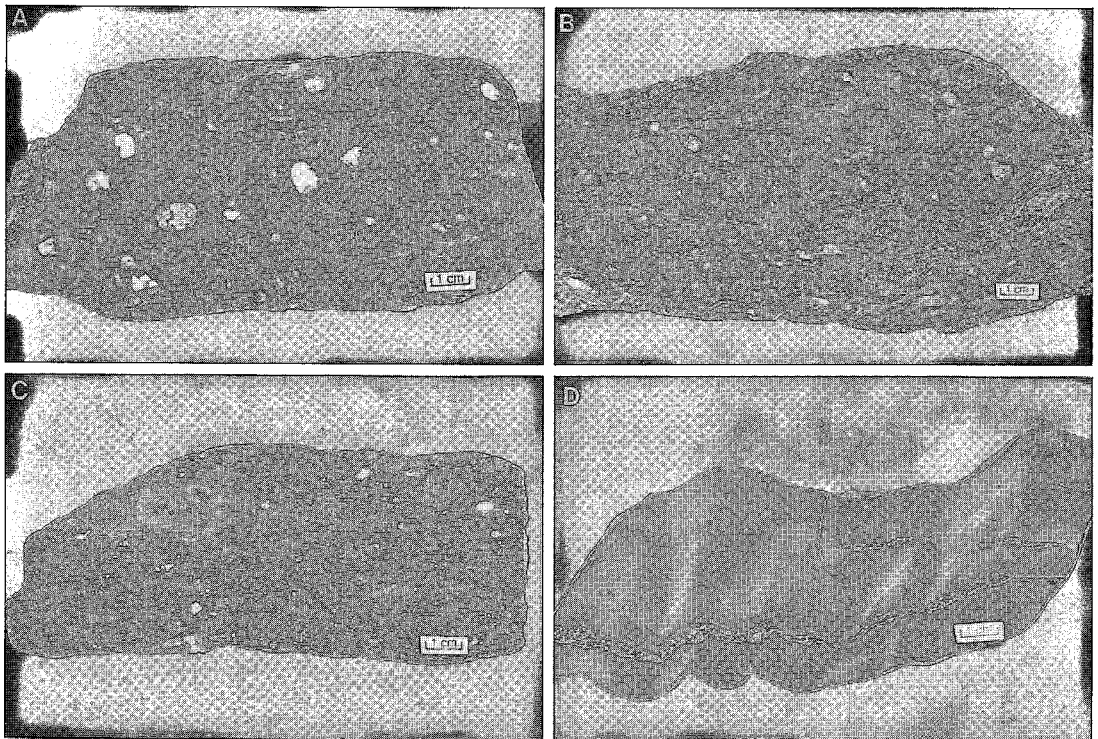
FIG. 4. Polished rock slabs from the 850-m level illustrating the progessive breakdown of coarse alkali feldspar phenocrysts with an increase in intensely foliated chlorite and sericite domains A) least-altered coarse-grained crystal-rich tuff (quartz–feldspar augen schist, QFAS; sample 012) from near No. 3 shaft; B) weakly altered coarse-grained crystal-rich tuff (quartz–(feldspar) augen schist, Q(F)AS; sample 153) with intermediate stages of replacement of alkali feldspar by albite, sericite, and Mg-rich chlorite, with disseminated and vein sulfides; C) moderately altered crystal-rich tuff (quartz-augen schist, QAS; sample 154), with quartz–sericite pseudomorphs of alkali feldspar, increase in content of Fe-rich mica, and strong development of a composite S_1 and S_2 penetrative fabric; D) moderately altered footwall sedimentary rock (FW) (sample 156), with a well-developed S_1 and S_2 fabric, and with transposed quartz–pyrrhotite veins.

The Nepisiguit Falls Formation consists of quartz–feldspar augen schist (QFAS), quartz–augen schist (QAS) or quartz-eye schist (QES), quartz–feldspar crystal tuff (CT) and sedimentary rocks (FW). These are descriptive terms that have long been used by geologists at Brunswick Mines (Fig. 2). The nomenclature has been revised in order to reflect the current understanding of the origin of these rock types.

Unfortunately, there are no series of samples that characterize the complete transition from the least-altered QFAS to the most-altered QAS in the core of the sulfide-stringer zone adjacent to the main ore-zone. The samples used in this study are from the flank of the main sulfide-stringer zone where there is good geological control along the entire sample profile. The 850- and 750-meter levels of the mine (Figs. 2A, B) were selected because they expose a virtually complete section of the QFAS–QAS transition through the Nepisiguit Falls Formation between the No. 3 shaft

and the footwall sedimentary rocks (Figs. 2A, B, 3, 4). The QAS unit is thin on this level, and the QFAS represents the "least-altered" footwall in the vicinity of the mine (sample 012) on the basis of preservation of primary textures, the presence of only weakly altered alkali feldspar and the weak penetrative fabric within the rock. Sample 012 was used as the basis for comparisons with all other samples. A sample of the footwall sedimentary rock (FW) (Fig. 4D), which directly overlies the QAS unit, was included in the two profiles in order to illustrate how the extent of alteration changes toward the sulfide body and across the QAS–FW contact. On the 850-m level, the contact between the QAS and FW is sharp and possibly depositional, whereas the same contact on the 750-m level is faulted, with late quartz veins occurring along the fault (Fig. 3). Localized alteration (<1 m wide) associated with the fault zone was avoided during sampling.

Coarse-grained crystal-rich tuff (QFAS)

The least-altered, crystal-rich tuffs (QFAS) are composed of coarse-grained turbid alkali feldspar, albite, and quartz phenocrysts that are hosted by a very fine-grained matrix of sericite, Mg-rich chlorite, albite, and opaque phases. The feldspar phenocrysts are subhedral to euhedral, and generally twice the size of the "vitreous" quartz grains. The feldspar crystals comprise 5 to 20 vol. % of the rock and are matrix-
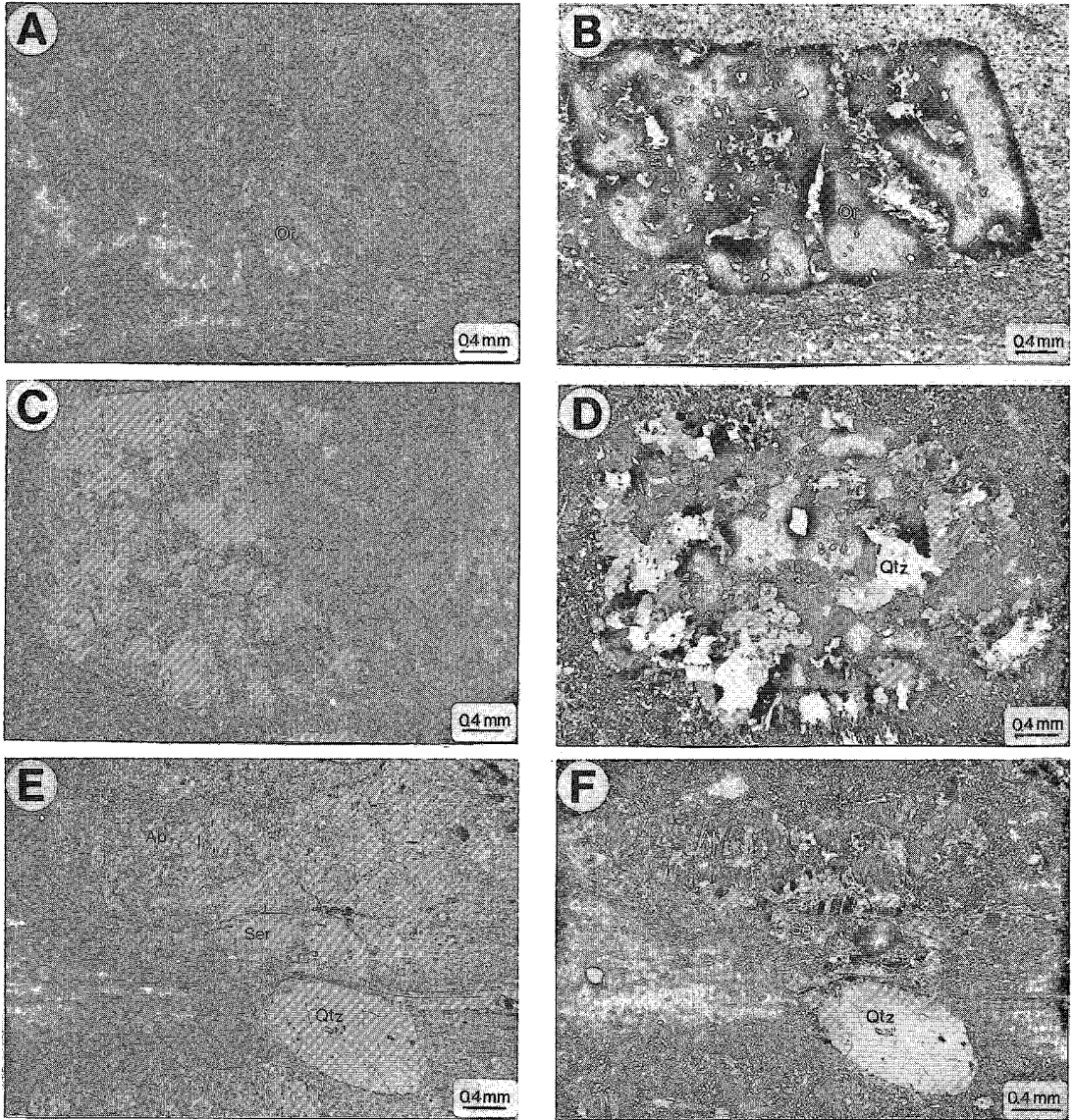
FIG. 5. Progressive alteration of feldspar in the crystal-rich tuffs (QFAS to QAS) beneath the Brunswick No. 12 massive sulfide deposit. A, B) Photomicrographs of phenocrysts of turbid alkali feldspar with fracture or pull-apart features filled with an assemblage of quartz – albite – chlorite (QFAS, sample 012, No. 3 shaft, 850-m level). Plane-polarized light (PP) in A and cross-polarized light (CP) in B. C, D) Photomicrographs of altered phenocryst of alkali feldspar composed of intergrown quartz and albite (chessboard) within the transition zone between QFAS and QAS (sample 009, 750-m level) (PP in C and CP in D. E, F) Photomicrograph of porphyroclast of secondary chessboard albite altered to sericite, quartz and partially deformed cataclastically within the QAS (sample 006, 750-m level) (PP in E and CP in F).

supported in most areas (Figs. 4A, B, C, 5A, B). The range in abundance of feldspar (10–20 vol. %) and quartz (20–30 vol. %) phenocrysts is consistent throughout the QFAS. There is overwhelming evidence for a volcanic origin for some of the quartz augen, including "vitreous" (black) quartz (paramorphs after β quartz), crystal shards, and amoeboid quartz. Paramorphs after β quartz were observed in the QFAS near the transition into QAS. Discontinuous dark grey to green wisps are morphologically similar to relict pumice and lithic fragments that have been observed in a few weakly deformed, coarse-grained units of the crystal tuff. Although not common, small dark grey to black wisps (0.5 to 1 cm, 10 vol. %) that resemble lithic fragments of metapelite were identified in the QAS and QFAS at the north end of the deposit. In some samples, alkali feldspar phenocrysts are cut and partly replaced by microcrystalline quartz – albite – chlorite – sericite veinlets, although the rock remains recognizable as QFAS. The minimal amount of crystal fragmentation, the absence of flow-top breccias, and the rare presence of fiamme are consistent with the QFAS originating as a submarine pyroclastic flow (Nelson 1983, Lentz & Goodfellow 1992a).

Fine-grained crystal-rich tuff (CT)

In the vicinity of the Brunswick No. 12 and 6 deposits, fine-grained quartz and feldspar, crystal-rich tuff (tuffite?) is laterally continuous but of variable thickness. The crystals are locally graded but usually homogeneously distributed in a glassy to granular matrix. Juras (1981), Nelson (1983), and Luff *et al.* (1992) have described fragmented crystals, relict fiamme, lithic fragments (0 to 20%), pumice clasts (10 to 20%), and granophyric textures in the crystal tuff. The absence of these textures in the stratigraphically lower QFAS is evidence against a reworking of the QFAS and QAS to form the fine-grained crystal-rich tuff (*cf.* Nelson 1983). This observation suggests that in places, the crystal tuff represents several reworked, distal pyroclastic fall deposits (Lentz & Goodfellow 1992a). This unit is also altered in the vicinity of the deposit, although the unit remains known as crystal tuff because of the difficulty in recognizing altered feldspar phenocrysts. Although this unit was not intersected in either profile sampled in this study, the footwall sedimentary rocks (FW) described below have some crystal-rich portions, indicating a derivation of components from this unit.

Footwall sedimentary rocks (FW)

There are several very fine-grained, moderately to poorly layered, leucocratic sedimentary rocks (FW) (mudstones) that occur in the footwall sequence of the Brunswick No. 12 deposit (Fig. 4D). The footwall sedimentary rocks occur directly beneath most of the deposit, and pinch out laterally into fine-grained crystal-rich tuff north and south of the deposit. The transition is quite sharp, possibly representing onlapping onto the crystal tuff or a lateral change in facies. Within the footwall sedimentary rocks, scattered fine-grained quartz and feldspar crystals and intercalated crystal tuffs indicate a variable pyroclastic component.

ALTERED FOOTWALL LITHOTYPES

The fine- to medium-grained altered crystal tuff, which is better known as quartz-augen schist (QAS), is composed of 20 to 30 vol. % subrounded to subangular grains or composite grains of quartz (± feldspar and mica) that are hosted in a dominantly sericitic matrix (Fig. 4C). Quartz grains range from 0.1 to 1 cm in diameter, and are matrix-supported and uniformly distributed. Small grains of mottled feldspar that are replaced by fine-grained mica or albite (or both) occur near the base of the QAS (Figs. 2A, B). The alkali feldspar phenocrysts decrease in abundance and size (0.2 to 2 cm) in the transition zone [Q(F)AS] between the QFAS and the QAS at the deposit. The stratigraphic thickness of the quartz-augen schist is variable (50 to <300 m) transgressing the stratigraphy, with both sharp (50 cm) and gradational (>100 m) transitions into QFAS. Granoblastic quartz, albite, sericite, and Fe–Mg-bearing chlorite have pseudomorphically replaced alkali feldspar phenocrysts (Figs. 5C, D) or albitized equivalents. Within the QAS, the alkali feldspar phenocrysts that are totally replaced by microcrystalline granoblastic quartz, sericite, and chlorite resemble milky quartz augen in hand specimen, unlike the "vitreous" angular to euhedral volcanic quartz that also is present. The diameter of the quartz augen in the QAS is generally 1 to 2 mm less than quartz augen in QFAS, whereas feldspar in the latter is up to twice as large as quartz. The smaller grain-size of the mica–quartz pseudomorphs compared to the original feldspar phenocrysts is attributed to either 1) preferential growth of mica on the margin of the quartz-rich pseudomorph, or 2) modification of the proportions of quartz and mica in the pseudomorph during recrystallization of the microcrystalline quartz to produce a more micaceous margin. The mineralogy and textural complexity of the pseudomorphs is important to consider the account of compositional changes, as pointed out by Gresens (1967).

Around the hinge zone of the F_1–F_2 sheath-like fold, the change in facies from footwall sedimentary rocks to the fine-grained crystal-rich tuffs coincides with zones of stringer-sulfide mineralization and associated intense hydrothermal alteration probably localized along a fault (Luff *et al.* 1992). High abundances of Fe-rich chlorite near the deposit have been attributed to either hydrothermal sedimentation during a pre-ore hydrothermal stage (McCutcheon 1990, 1992) or to pervasive chloritic alteration (melanocratic) by

hydrothermal fluids that have migrated laterally from the hydrothermal vent (stringer-sulfide zone) (Goodfellow 1975a, b, Jambor 1979, Juras 1981, Nelson 1983, Luff et al. 1992). The latter process would have chloritized and sericitized the footwall units (Fig. 4).

The S_1 and S_2 fabrics are commonly more pronounced in the QAS and FW than in the QFAS by virtue of the higher content of phyllosilicates in the matrix (i.e., less cryptocrystalline feldspar in the matrix) and the absence of feldspar phenocrysts. The well-developed fabrics indicate that deformation may, in part, be responsible for the fragmentation of the phenocrysts, resulting in a finer grain-size. Many phenocrysts have variably developed deformation-related, fine-grained mica–quartz beards in their pressure shadows that have mineralogical and textural attributes similar to those in pull-apart structures (cf. van Staal 1985), although these features probably represent local in situ recrystallization of the matrix, because the phenocrysts are not affected in many cases. Despite the localized effects of deformation, the morphological preservation of some of the pseudomorphs is compelling evidence for a pre-deformational origin. In addition, the minimal alteration in the post-ore, synvolcanic composite mafic to felsic quartz–feldspar porphyry dike that cuts the QAS to the south of the deposit (Fig. 2A) indicates that alteration preceded dike emplacement and, therefore, deformation (Lentz & van Staal 1992). The pre-dike replacement of alkali feldspar phenocrysts supports the contention that the QAS is a product of alteration of the QFAS (Goodfellow 1975a, Juras 1981, Nelson 1983, Lentz & Goodfellow 1992a, Luff et al. 1992). The occurrence, therefore, of milky quartz-augen pseudomorphs with "vitreous" volcanic quartz is evidence of submarine hydrothermal alteration and may explain the common association of QAS with felsic volcanic-hosted massive sulfide deposits.

Petrography

Feldspars

Within the least-altered crystal-rich pyroclastic rocks, turbid alkali feldspar and albite phenoclasts have been identified. Rare microperthitic textures are preserved (Nelson 1983). The coarse-grained alkali feldspar phenoclasts are irregularly turbid and commonly exhibit authigenic overgrowths that are colorless and free of inclusions (i.e., not turbid). The alkali feldspar phenoclasts have no albite lamellae and are low in Na, indicating either diagenetic, hydrothermal or upper-greenschist metamorphic alteration of the felsic pyroclastic rocks (Table 1). These features have been described in keratophyres in submarine pyroclastic rocks (Munhá et al. 1980). The celsian component of the feldspar is quite low and irregular, possibly because of the effects of hydrothermal alteration (cf.

Hughes 1973). The barium content of the alkali feldspar is consistent with the whole-rock abundances observed in the least-altered rocks. Detailed X-ray analyses of feldspar separates indicate that the alkali feldspar consists of ordered microcline, although some crystals or portions of crystals are slightly more disordered and may be authigenic (Juras 1981, Nelson 1983). At the Brunswick No. 6 deposit, Nelson (1983) determined that the degree of Si–Al order within the feldspar was probably related to diagenetic reaction with seawater and was not spatially related to the hydrothermal alteration, although a metamorphic origin cannot be ruled out.

Two morphological types of plagioclase occur in the least-altered rocks, small euhedral laths of primary plagioclase (albite) and secondary albite or secondary chessboard albite irregularly replacing alkali feldspar or primary plagioclase. Both varieties of albite typically contains a negligible amount of the An component ($Ab_{99}An_1$, Table 1), which is indicative of re-equilibration under greenschist-grade metamorphic conditions or possibly through alteration by seawater. They also have uniformly low K, Sr, and Ba contents (Table 1). In other areas of the Bathurst Camp, secondary albite, including chessboard varieties, also have formed (Starkey 1959) probably at the expense of the microcline phenoclasts. Chessboard albite has been described in association with keratophyric alteration (Battey 1955) in other submarine volcanic settings.

Phyllosilicates

The composition of mica was determined in selected samples to characterize mineralogical variations and mineral zonation related to alteration and to support mass-balance calculations. Electron-microprobe analyses of mica in the least-altered rocks (QFAS) were difficult to obtain because of the fine grain-size. Analyses of mica in QFAS from the 750-m level were supplemented with data from the stratigraphically equivalent footwall sedimentary rock (sample 156), 850-m level. Total iron was represented as Fe^{2+}, as supported by the presence of low-$f(O_2)$ sulfide assemblages (pyrrhotite–chalcopyrite) in the footwall. In addition, the average d_{060} value in chorite is 1.555 Å, which is equivalent to a b_0 of 9.33 Å (Juras 1981). The large b_0 of chlorite is additional evidence that the chlorite is reduced (high Fe^{2+}) (cf. Brindley & Youell 1953). The prominent 14 Å d_{001} peak in the footwall samples examined by Juras (1981) indicates these samples have negligible septechlorite, consistent with re-equilibration to the upper greenschist metamorphic grade. However, this does not rule out the original presence of septechlorite in the assemblage attributed to premetamorphic alteration, especially since both pre- and postmetamorphic berthierine was identified in the alteration zone at the Kidd Creek deposit (Slack et

al. 1992).

The composition of chlorite ranges from pycnochlorite in QFAS to ripidolite in the QAS and footwall sedimentary units (*cf.* Hey 1954; Table 2) similar to the range identified by Luff *et al.* (1992). Average compositions of mica were calculated for each sample to smooth the irregular and overprinting effects of alteration. The coexisting intergrown sericite has a component of phengite. In both chlorite and sericite, there is a slight decrease in ^{IV}Si and an increase in ^{IV}Al and ^{VI}Al from the least-altered (sample 012) to the most altered (sample 156) rock (Figs. 6A, B). Tschermak substitution ($^{IV}Si + {}^{VI}R \rightleftharpoons {}^{IV}Al + {}^{VI}Al$) results in the positive correlation between ^{IV}Al and ^{VI}Al. However, at low Al contents, a coupled substitution involving Si and Mg predominates, whereas at

higher total Al contents, Si and Fe are favored. This is responsible for the enrichment in ^{IV}Al and ^{VI}Al with increasing Fe/(Fe+Mg) ratio (Fig. 6). This effect is due to crystal-chemical considerations (*cf.* Kranidiotis & MacLean 1987), possibly because the Fe^{2+} ion can substitute more readily with an increase in ^{IV}Al in the chlorite or because Al readily substitutes for Mg in the "brucite" layer (Deer *et al.* 1962). The covariance between Fe/(Fe+Mg) and Al content also is probably enhanced by the compositional variations produced by changing activities of Si, Al, Fe, and Mg in the hydrothermal fluid, for example, the enrichment in Al and Fe in the protolith toward the massive sulfide. At present, the respective contributions of each of these factors remains unconstrained. The compositional changes are, nevertheless, consistent with the leaching

TABLE 1. AVERAGE FELDSPAR COMPOSITIONS FROM HYDROTHERMALLY ALTERED, CRYSTAL-RICH FELSIC PYROCLASTIC ROCKS, 750 m LEVEL BRUNSWICK NO. 12 MASSIVE SULFIDE DEPOSIT, BATHURST, NEW BRUNSWICK

Sample	012		012	009		009		008		007	
Host	QFAS		QFAS	QFAS		QFAS		QFAS		QAS	
Mineral	Mc		Ab	Mc		Ab		Ab		Ab	
No.	5	1s	1	8	1s	3	1s	4	1s	4	1s
SiO₂ wt.%	64.3	0.8	66.5	62.5	0.4	67.7	0.5	67.3	0.4	67.5	0.5
TiO₂	0.04	0.05	0.00	0.04	0.06	0.10	0.09	0.05	0.05	0.03	0.06
Al₂O₃	19.22	0.36	19.55	18.71	0.14	20.2	0.35	19.90	0.10	19.95	0.20
Fe₂O₃T	0.05	0.02	0.12	0.07	0.08	0.02	0.03	0.03	0.03	0.07	0.06
MgO	0.04	0.02	0.00	0.03	0.01	0.03	0.03	0.00	0.00	0.02	0.01
MnO	0.01	0.01	0.02	0.01	0.01	0.04	0.03	0.03	0.03	0.02	0.02
BaO	0.53	0.31	0.13	0.46	0.42	0.23	0.20	0.12	0.18	0.03	0.04
CaO	0.04	0.07	0.00	0.01	0.01	0.21	0.15	0.06	0.01	0.04	0.02
SrO	0.05	0.02	0.00	0.06	0.03	0.00	0.00	0.00	0.00	0.00	0.00
Na₂O	0.18	0.07	11.55	0.26	0.05	11.98	0.05	12.10	0.31	11.96	0.18
K₂O	15.31	1.26	0.21	16.54	0.14	0.13	0.03	0.10	0.03	0.04	0.01
Total	99.7		98.1	98.6		100.6		99.7		99.7	
Si	2.98		2.97	2.96		2.96		2.96		2.97	
Al	1.05		1.03	1.04		1.04		1.03		1.03	
Fe3+	0.00		0.00	0.00		0.00		0.00		0.00	
Mn	0.00		0.00	0.00		0.00		0.00		0.00	
Mg	0.00		0.00	0.00		0.00		0.00		0.00	
Ba	0.01		0.00	0.01		0.00		0.00		0.00	
Ca	0.00		0.00	0.00		0.01		0.00		0.00	
Na	0.02		1.00	0.02		1.01		1.03		1.02	
K	0.90		0.01	1.00		0.01		0.01		0.01	

* Notes: Mineral formulas were calculated assuming 8 atoms of oxygen. The presence of micaceous inclusions results in high aluminum and low alkalis. The least altered sample 012 is located 350 m from footwall metasediments (FW), 009 (50 m from FW), 008 (30 m from FW), 007 (15 m from FW), 006 (1 m from FW), 156 (5 m from QAS). QFAS = quartz-feldspar-augen schist (least-altered crystal-rich tuff); QAS = quartz-augen schist (altered crystal-rich tuff). Mc (microcline) and Ab (albite). No. = number of analyses used to calculate average composition; 1s = 1 standard deviation. Chemical analyses were obtained at the Geological Survey of Canada using a Cameca 1electron microprobe (WDS) at 15 kV and 9.5 μamps operating current and calibrated with feldspar standards.
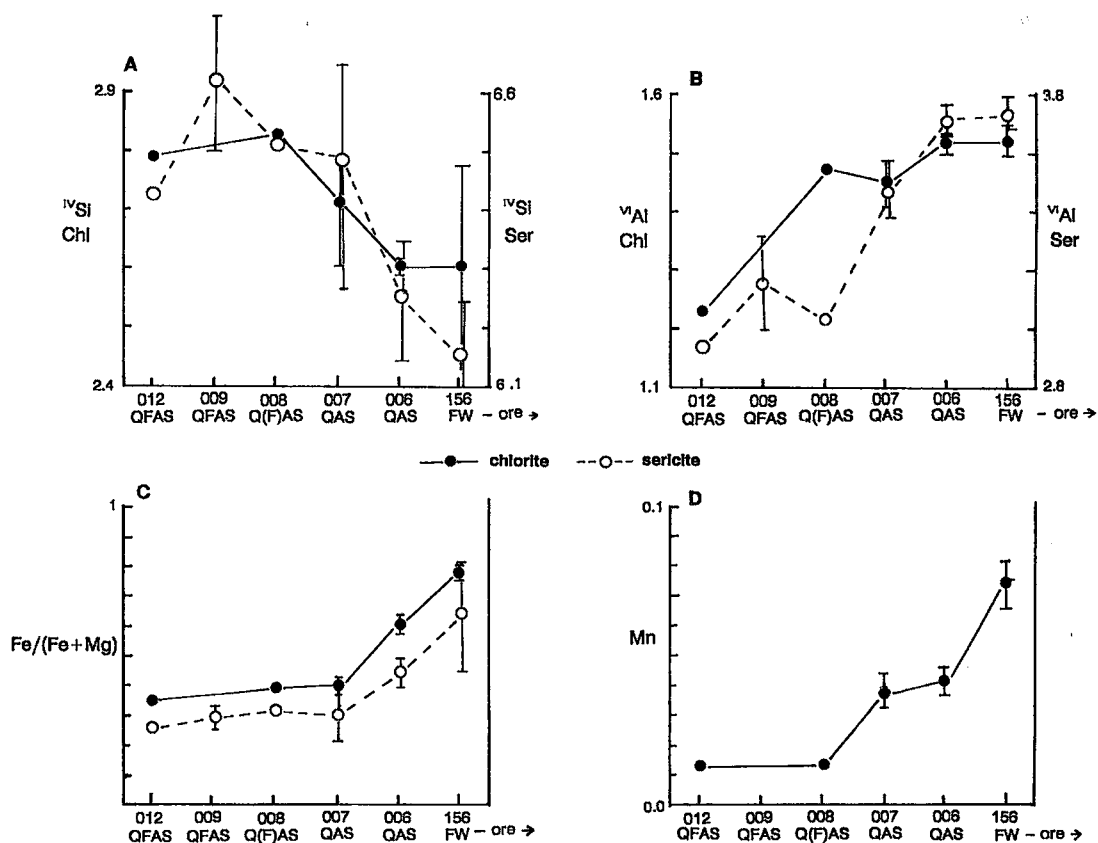
FIG. 6. Compositional variation in chlorite and sericite from the least-altered crystal-rich tuffs (QFAS) to altered crystal-rich tuffs into the altered footwall sedimentary rocks (FW) as a function of distance along the sample profiles toward ore zone (Table 2). A) ^{IV}Si content *versus* distance, B) ^{VI}Al content *versus* distance, C) Fe/(Fe+Mg) *versus* distance, and ^{VI}Mn *versus* distance. Error bars represent 95% confidence intervals ($\pm = t_{0.025}s/\sqrt{n}$ is a 95% confidence interval: Le Maitre 1982).

of alkali constituents from the rock to form a more aluminous residuum, and the increase in Fe/(Fe+Mg) in the mica toward the more intensely altered zone beneath the ore deposit (Fig. 6C). The Mn^{2+} content of chlorite also increases with Fe in the more altered rocks (Fig. 6D). The chlorite compositions substantiate previous observations of the vent-proximal Mg–Fe chlorite (richer in Fe) and vent-distal Fe–Mg chlorite (richer in Mg) described by Luff *et al.* (1992). Similar compositional variations have been observed in chlorite from several other massive sulfide deposits of the Bathurst Camp (Sutherland 1967, Jambor 1981, Lewczuk 1990).

In recent years, some studies of alteration have documented Fe enrichment in chlorite toward the core of the hydrothermal system (*e.g.*, Roberts & Reardon

1978, Hendry 1981, McLeod & Stanton 1984, Kranidiotis & MacLean 1987, Slack & Coad 1989, Leitch 1992, Luff *et al.* 1992, Slack *et al.* 1992, Cameron *et al.* 1993), although few have correlated this enrichment with the composition of coexisting phengitic mica (Hendry 1981, Cameron *et al.* 1993). The positive correlation of the Al content of chlorite and phengitic sericite with the Fe/(Fe+Mg) content of these minerals is probably a function of the differences in bulk composition produced by alteration, as these rocks have been uniformly metamorphosed to upper-greenschist-grade conditions. The Al content of phengitic mica is variable, and therefore incapable of "buffering" the Al content of chlorite to a fixed composition as a function of temperature. The proposed chlorite geothermometer (*cf.* Cathelineau & Nieva

TABLE 2. AVERAGE PHYLLOSILICATE COMPOSITIONS FROM HYDROTHERMALLY ALTERED, CRYSTAL-RICH FELSIC PYROCLASTIC ROCKS, 750 m LEVEL BRUNSWICK NO. 12 MASSIVE SULFIDE DEPOSIT, BATHURST, NEW BRUNSWICK

Sample	012	012	009	009	008	008	007	007	007	007	006	006	006	006	156	156	156	156
Host	QFAS	QFAS	QFAS	QFAS	Q(F)AS	Q(F)AS	QAS	QAS	QAS	QAS	QAS	QAS	QAS	QAS	FW	FW	FW	FW
Mineral	Chl	Ser	Ser		Chl	Ser	Chl		Ser		Chl		Ser		Chl		Ser	
No.	1	1	4	1s	1	2	4	1s	4	1s	7	1s	8	1s	10	1s	9	1s
SiO_2 wt.%	26.9	45.9	47.9	0.8	25.7	46.4	25.6	0.7	48.7	1.41	23.3	0.2	47.1	0.8	23.20	1.81	46.13	0.95
TiO_2	0.07	0.31	0.34	0.04	0.13	0.33	0.30	0.30	0.30	0.29	0.04	0.06	0.27	0.11	0.08	0.07	0.22	0.04
Al_2O_3	19.93	27.31	27.78	1.16	20.47	27.3	22.02	0.47	31.9	0.7	22.16	0.22	34.9	0.5	21.99	0.68	35.58	0.61
FeO	20.08	3.08	2.16	0.20	16.89	3.01	19.84	0.44	1.71	0.40	28.5	1.3	1.46	0.28	35.53	0.59	2.24	1.11
MgO	19.33	4.81	2.88	0.09	17.14	3.58	16.88	2.27	2.27	0.38	10.11	0.24	1.05	0.08	5.75	0.13	0.70	0.28
MnO	0.14	0.01	0.02	0.02	0.13	0.04	0.39	0.06	0.04	0.04	0.41	0.05	0.02	0.02	0.75	0.10	0.03	0.04
CaO	0.04	0.02	0.05	0.04	0.02	0.03	0.04	0.04	0.02	0.01	0.00	0.02	0.03	0.03	0.01	0.02	0.03	0.04
SrO	0.00	0.05	0.03	0.03	0.02	0.00	0.03	0.01	0.03	0.01	0.06	0.00	0.08	0.02	0.01	0.02	0.03	0.04
BaO	0.00	0.09	0.04	0.08	0.00	0.00	0.00	0.01	0.28	0.29	0.00	0.00	0.12	0.08	0.01	0.17	0.15	0.58
Na_2O	0.00	0.33	0.04	0.04	0.00	0.00	0.00	0.01	0.22	0.05	0.00	0.00	0.35	0.08	0.00	0.02	0.09	0.15
K_2O	0.05	10.18	10.88	0.52	0.01	10.75	0.05	0.09	9.09	0.05	0.08	0.05	9.80	0.46	0.12	0.11	9.40	0.58
H_2O	11.61	4.28	4.34		11.93	4.13	11.64		4.41		11.12		4.32		10.76		4.33	
F	0.32	0.30	0.27	0.03	0.53	0.24	0.25	0.17	0.21	0.02	0.42	0.17	0.17	0.03	0.35	0.17	0.35	0.17
Cl	0.02	0.03	0.02	0.02	0.12	0.02	0.02	0.02	0.02	0.01	0.02	0.01	0.01	0.01	0.03	0.03	0.03	0.02
O=F	0.13	0.13	0.11		0.22	0.10	0.10		0.11		0.09		0.18		0.07		0.15	
O=Cl	0.00	0.01	0.00		0.03	0.00	0.00		0.01		0.00		0.07		0.01		0.01	
Total	98.3	96.5	96.9		96.5	96.7	96.7		99.1		95.9		99.7		98.4		99.6	
Fe /(Fe + Mg)	0.37	0.26	0.30		0.36	0.32	0.40		0.30		0.61		0.44		0.78		0.64	
Si	2.79	6.43	6.63		2.82	6.52	2.71		6.48		2.60		6.25		2.61		6.15	
^{IV}Al	1.21	1.57	1.37		1.18	1.48	1.29		1.52		1.40		1.75		1.39		1.85	
^{VI}Al	1.23	2.94	3.17		1.47	3.03	1.45		3.49		1.52		3.71		1.52		3.74	
Ti	0.01	0.03	0.04		0.01	0.03	0.00		0.03		0.00		0.03		0.01		0.02	
Fe2+	1.74	0.36	0.25		1.55	0.35	1.76		0.19		2.66		0.16		3.34		0.25	
Mn	0.01	0.00	0.00		0.01	0.00	0.03		0.00		0.04		0.00		0.07		0.00	
Mg	2.99	1.00	0.59		2.80	0.75	2.66		0.45		1.69		0.21		0.96		0.14	
Ba	0.00	0.00	0.00		0.00	0.00	0.00		0.01		0.00		0.01		0.00		0.02	
Ca	0.00	0.00	0.01		0.00	0.01	0.01		0.00		0.00		0.00		0.00		0.00	
Na	0.00	0.09	0.01		0.01	0.06	0.00		0.01		0.00		0.09		0.02		0.10	
K	0.01	1.82	1.92		0.00	1.93	0.01		1.54		0.01		1.66		0.02		1.60	
OH	7.89	3.86	3.88		7.99	3.74	7.92		3.89		7.92		3.82		7.93		3.84	
F	0.10	0.13	0.12		0.23	0.11	0.08		0.11		0.07		0.18		0.06		0.15	
Cl	0.00	0.01	0.00		0.08	0.00	0.01		0.01		0.00		0.02		0.01		0.01	
Oxygens	14	20	20	20	14	20	14	14	20	20	14	14	20	20	14	14	20	20

* Notes: The least-altered sample 012 is located 350 m from footwall metasediments (FW), 009 (50 m from FW), 008 (30 m from FW), 007 (15 m from FW), and 006 (1 m from FW). QFAS = quartz-feldspar- augen schist (least-altered crystal-rich tuff); QAS = quartz-augen schist (altered crystal-rich tuff); FW = footwall sedimentary rocks. Chl (chlorite) and Ser (sericite). No. = number of analyses used to calculate average composition; 1s = 1 standard deviation about the mean. Chemical analyses of very fine-grained intergrown chlorite and sericite was problematic, particularly in the QFAS; therefore, only selected results are reported. Chemical analyses were obtained at the Geological Survey of Canada using a Cameca electron microprobe (WDS) at 15 kV and 9.5 μamps operating current and calibrated with mica and amphibole standards. Some low totals are probably due to the very-fine-grained nature of the micas in the least-altered samples. Mineral formula and H_2O were calculated with MINFILE, a program created by A. Afifi and E. Essene at the University of Michigan, Ann Arbor, Michigan, U.S.A.

1985, Kranidiotis & MacLean 1987) is not applicable to rocks that have undergone metamorphism at the middle to upper greenschist grade at higher pressures because the celadonite content of sericite increases with increasing pressure (Massonne & Schreyer 1987). A minimum $P(H_2O)$ estimate of 600 to 650 MPa (6.0 –6.5 kbar) is indicated by Fe–Mg-bearing phengite compositions in samples with the critical quartz – chlorite – K-feldspar ($\pm$ phlogopite) assemblage, which is supported by sphalerite geobarometry (van Staal 1985, Lentz & Goodfellow 1993b). The close correlation between the compositions of chlorite and phengitic sericite indicates that they represent an equilibrium assemblage because major-element distributions between coexisting minerals are a function of temperature, pressure, and variations in other major elements. The coexisting chlorite and white mica, therefore, have the potential of testing for equilibrium between mineral phases (Kretz 1959).

$$[Fe]\ K_D^{Chl/Ms} = [X_{Fe}^{Chl}(1-X_{Fe}^{Ms})]/$$
$$[(1-X_{Fe}^{Chl})X_{Fe}^{Ms}] \hspace{2cm} [1]$$

where [Fe] = Fe/(Fe+Mg) for K_D, and X_{Fe} = Fe/(Fe+Mg).

The distribution coefficients (K_D) of Fe/(Fe+Mg) have been calculated for averaged chlorite and phengite data from each sample set. The [Fe] $K_D^{Chl/Ms}$ is 1.68 ($n = 5$). The slightly irregular distribution of [Fe] between chlorite and phengite is probably due to the effect of Al variation in sericite and chlorite. This is similar to the K_D calculated for a chlorite–sericite pair from the Kidd Creek VMS deposit ($K_D^{Chl/Ms}$ between 2.0 and 2.5, Cameron *et al.* 1993). In an examination of the altered rocks around the Prince Lyell massive sulfide deposit, Hendry (1981) noted that the distribution of Fe/(Fe+Mg) between chlorite and phengite, [Fe] $K_D^{Chl/Ms}$, is approximately equal to 1, although he attributed the distribution to diagenetic–hydrothermal features and not to re-equilibration during greenschist-grade metamorphism. In a study of structurally deformed low-grade, greenschist-grade pyroclastic rocks, Ramamohana Rao (1977) found that chlorite and phengite had re-equilibrated during metamorphism (recalculated [Fe] $K_D^{Chl/Ms} = 0.65 \pm 0.19$) indicating that, in this case, the phengite has a higher X_{Fe} than the coexisting chlorite. With all else being equal with increasing metamorphic grade, the Fe/(Fe+Mg) distribution between chlorite and phengite increases with metamorphic grade. Nonetheless, the mica compositions in low-grade metamorphic rocks should still reflect the bulk composition of the altered parent rock (*cf.* Ramamohana Rao 1977, Hendry 1981, McLeod & Stanton 1984, Kranidiotis & MacLean 1987). In this study, for example, the Pearson product correlation coefficient of Fe/(Fe+Mg) in chlorite and phengite *versus* the bulk-rock composition ($r = 0.85$ and 0.92, respectively, Le Maitre 1982) is high (>95% confidence level) and may be used as a mineralogical index of alteration.

It is well known that high fugacities of reduced S_2 and CO_2 can affect the composition of silicates coexisting with carbonate or sulfides or both. Within the zone of footwall alteration, the ubiquitous presence of pyrite and lesser proportions of pyrrhotite, sphalerite, chalcopyrite and, more rarely, siderite with chlorite and phengite indicate that $f(S_2)$ and $f(CO_2)$ should be considered as important variables. Despite the moderate to high $f(S_2)$ and $f(CO_2)$, the chlorite and phengite in the proximal altered rocks still have a high Fe/(Fe+Mg) value compared to those in the more distal alteration [Q(F)AS and QFAS] facies. Two additional factors also must be considered: 1) there may be a compositional limit to the Fe/(Fe+Mg) ratio at a given Al content, and 2) a decrease in divalent metals at the expense of Al may coincide with an increase in the Fe/(Fe+Mg) ratio regardless of high $f(S_2)$ and $f(CO_2)$. Until crystal-chemical controls are fully understood, caution must be used in interpreting chemical variations in chlorite and phengite as a function of variations in activities of hydrothermal components.

MASS-BALANCE CONSTRAINTS

The chemical composition of the QFAS, QAS, and several FW rocks was determined along two sample profiles (Figs. 2A, B, Table 3). Mass-balance calculations were carried out to identify the chemical changes resulting from alteration of the least-altered QFAS to the moderately altered QAS (Table 4). The major- and trace-element composition of the least-altered QFAS (sample 012) used in these mass-balance calculations is very similar to the other QFAS units in the Bathurst Camp (*cf.* Lentz & Goodfellow 1992b). The variable MgO content (1–3 wt.%) and variable Na_2O and K_2O contents are consistent with keratophyric alteration of the subaqueous felsic pyroclastic sequence (*cf.* Hughes 1973).

Enrichment–depletion ratios for the elements are calculated by correcting for the changes in volume by comparing with a least-altered parent (*cf.* Gresens 1967). The difference between this recalculated value of the altered rock and least-altered parent was determined and divided by the value of the least-altered parent to yield a relative variation that can then be converted to a percentage.

The natural variation in the crystal-matrix ratio in these pyroclastic and reworked pyroclastic rocks makes it essential to rely on Al as the immobile element because it occurs in both the crystals and the matrix. The variation in the proportion of the matrix (60 to 80%) is reflected by highly variable trace-element contents compared to that for pristine igneous rocks. Aluminum is also considered relatively immobile under these hydrothermal and greenschist-grade metamorphic conditions. In an albite – paragonite –

TABLE 3. MAJOR- AND TRACE-ELEMENT COMPOSITIONAL DATA FROM TWO SECTIONS THROUGH THE CRYSTAL-RICH TUFF ON THE 850 m AND 750 m LEVELS OF THE BRUNSWICK NO. 12 MINE, NEW BRUNSWICK

Sample	012	150	151	152	153	154	155	156	009	008	007	006	005A	005B
Type	QFAS	QFAS	QFAS	QFAS	Q(F)AS	Q(F)AS	QAS	FW	QFAS	Q(F)AS	QAS	QAS	FW	FW
Level (m)	850	850	850	850	850	850	850	850	750	750	750	750	750	750
SiO_2 wt.%	69.5	71.1	69.0	69.9	60.3	67.5	70.0	65.3	69.4	71.1	65.8	60.3	70.0	44.7
TiO_2	0.55	0.60	0.58	0.59	0.45	0.53	0.62	0.45	0.56	0.56	0.57	0.66	0.40	0.54
Al_2O_3	14.3	13.9	14.1	14.1	11.6	12.7	14.6	12.1	14.1	13.5	14.1	16.0	8.30	9.49
Fe_2O_{3T}	3.60	3.40	3.90	3.60	12.4	7.00	3.90	14.3	4.00	4.80	6.60	11.5	11.9	25.8
Fe_2O_3	0.7	1.7	<0.2	0.9	-	-	0.7	-	-	-	0.6	1.3	-	-
FeO	2.6	1.5	3.6	2.4	-	-	2.9	-	-	-	5.4	9.2	-	-
MgO	3.28	1.65	1.79	2.10	1.98	2.40	2.87	1.37	1.91	2.08	4.41	3.32	1.67	1.16
MnO	0.03	0.04	0.07	0.07	0.08	0.04	0.04	0.21	0.04	0.05	0.09	0.15	0.23	0.14
CaO	0.33	0.31	0.36	0.32	0.33	0.21	0.20	0.17	0.20	0.22	0.30	0.20	0.21	0.42
Na_2O	1.10	1.30	1.90	1.60	1.02	0.80	0.80	0.10	0.90	0.80	0.70	0.10	0.20	0.15
K_2O	4.69	5.01	4.03	4.83	3.70	3.93	3.70	2.33	4.94	4.35	2.91	3.20	1.18	1.89
P_2O_5	0.18	0.18	0.19	0.18	0.15	0.17	0.18	0.16	0.17	0.18	0.19	0.18	0.18	0.26
H_2O	2.7	1.7	1.7	2.0	-	-	2.9	-	-	-	3.6	4.2	-	-
CO_2	0.0	0.2	0.19	0.1	2.5	0.4	0.2	<0.1	0.0	0.2	0.0	0.0	0.8	0.0
S	0.02	0.69	0.33	0.15	6.58	2.95	0.40	2.64	1.31	1.60	0.19	0.73	2.06	11.8
F ppm	822	1160	526	808	750	859	1116	720	726	1014	1379	1445	573	812
Cl ppm	296	146	437	151	253	<100	116	134	105	<100	220	366	<100	1180
Total	100.2	100.1	99.7	99.6	101.4	98.9	100.2	99.8	97.8	99.6	99.8	100.0	99.0	100.4
Fe/(Fe+Mg)	0.56	0.71	0.72	0.66	0.88	0.77	0.61	0.92	0.71	0.73	0.63	0.80	0.89	0.96
Ba ppm	730	690	460	630	350	450	260	270	690	460	220	240	130	230
Rb	130	150	140	160	-	120	130	38	150	130	110	140	<5	-
Sr	41	49	55	52	<20	23	25	21	23	18	26	25	18	12
Zr	270	250	270	260	200	250	270	130	270	250	280	300	91	200
Y	31	36	37	36	29	32	35	29	35	38	37	37	17	29
Nb	19	<10	18	<10	-	18	21	13	22	17	23	25	8	-
Be	2.1	1.6	1.9	1.7	1.6	1.7	2.4	1.2	1.9	1.8	2.2	2.7	0.5	1.0
Cu	5	19	17	11	120	27	12	200	12	22	9	22	890	2600
Pb	16	<20	38	<20	210	69	47	3900	18	63	64	76	3400	3600
Zn	69	65	120	120	460	230	190	1200	73	200	320	2300	13000	32000
As	11.7	0.4	3.4	5.0	6.6	17.0	7.4	94.7	12.4	24.7	28.1	6.7	45.3	2717
Bi	<0.2	0.5	0.2	<0.2	1.5	0.5	0.2	0.7	<0.2	0.2	1.8	1.0	0.5	1.8
Sb	0.9	0.3	4.3	0.7	16.2	3.0	2.0	26.9	2.3	2.7	2.0	17.8	10.8	51.7
Cr	17	22	20	21	22	21	21	<10	18	19	21	25	21	21
Ni	6	<10	10	<10	30	<10	11	12	4	8	10	11	11	83
Co	10	10	10	9	33	11	10	19	10	11	11	10	38	350
V	39	37	39	38	33	37	44	20	37	38	39	46	34	35
Sc	9.4	9.0	9.1	9.0	8.1	8.5	10.0	12.0	9.0	9.0	9.3	11.0	8.0	9.1
La ppm	48	49	51	45	41	48	50	36	44	49	45	55	29	57
Ce	86	100	110	94	87	100	100	74	94	100	95	120	68	120
Pr	15	13	12	11	10	12	12	8.5	11	12	11	13	6.7	12
Nd	41	49	48	43	40	47	48	34	43	46	44	54	28	49
Sm	11.0	10.0	9.9	8.9	8.3	9.4	9.8	6.9	8.4	9.0	8.8	11	5.6	9.4
Eu	2.1	1.3	1.3	1.2	1.4	1.3	1.4	5.1	1.3	1.6	1.5	1.7	2.9	4.9
Gd	7.6	10.0	10.0	9.4	7.6	8.2	8.7	6.3	8.3	8.7	8.6	11.0	5.7	10.0
Tb	1.3	1.4	1.3	1.2	1.2	1.3	1.3	1.0	1.3	1.3	1.3	1.5	0.67	1.2
Dy	6.8	8.1	8.1	7.7	6.9	7.4	7.9	6.2	8.0	8.1	8.2	8.4	3.9	6.6
Ho	1.3	1.6	1.5	1.4	1.4	1.4	1.5	1.3	1.6	1.6	1.6	1.6	0.72	1.2
Er	3.6	4.1	4.1	4.0	3.5	3.7	4.0	3.6	4.4	4.3	4.4	4.3	2.1	3.2
Tm	0.66	0.65	0.60	0.58	0.55	0.57	0.64	0.57	0.71	0.70	0.71	0.67	0.33	0.49
Yb	3.5	4.0	3.7	3.7	3.5	3.7	3.9	3.6	4.1	3.9	4.1	3.9	2.1	2.8
Lu	0.64	0.58	0.53	0.54	0.52	0.52	0.58	0.55	0.59	0.56	0.58	0.62	0.33	0.43
ρ	2.74	2.75	2.75	2.75	2.90	2.82	2.75	2.83	2.78	2.79	2.76	2.85	-	-

* Notes: QFAS: quartz–feldspar augen schist (least-altered crystal-rich tuff), QAS: quartz-augen schist (altered crystal-rich tuff), FW: footwall tuffaceous metasedimentary rocks. - denotes no analysis. All chemical analyses were carried out by the geochemistry staff of the Geological Survey of Canada. The concentration of major elements and selected trace elements (Ba, Rb, Sr, Nb, Y and Zr) was determined by X-ray fluorescence spectroscopy (XRF). Proportions of FeO, H_2O, CO_2, F, Cl, and S were determined by wet-chemical methods. Concentrations of the rare-earth elements were determined by inductively coupled plasma emission spectrometry (ICP–ES), whereas concentrations of the remaining trace elements were determined by inductively coupled plasma – mass spectrometry (ICP–MS). Analytical errors illustrated in the graphs were determined on duplicate analyses. The population variance for the QFAS was estimated from the average and standard deviation of six QFAS analyses from McCutcheon (1990).

TABLE 4. MASS-CHANGE DATA EXPRESSED AS A PERCENTAGE CHANGE ASSUMING Al-IMMOBILITY, FROM TWO SECTIONS THROUGH THE CRYSTAL-RICH TUFF ON THE 850 m AND 750 m LEVELS OF THE BRUNSWICK NO. 12 MASSIVE SULFIDE DEPOSIT, BATHURST, NEW BRUNSWICK

Sample	150	151	152	153	154	155	156	009	008	007	006	005A
Type	QFAS	QFAS	QFAS	Q(F)AS	Q(F)AS	QAS	FW	QFAS	Q(F)AS	QAS	QAS	FW
Level (m)	850	850	850	850	850	850	850	750	750	750	750	750
SiO_2	5.2	0.7	2.0	7.0	9.4	-1.4	11.0	1.3	8.3	-4.0	-22.5	73.5
TiO_2	12.2	7.0	8.8	0.9	8.5	10.4	-3.3	3.3	7.9	5.1	7.3	25.3
Al_2O_3	0	0	0	0	0	0	0	0	0	0	0	0
Fe_2O_{3T}	-2.8	9.9	1.4	325	119	6	369	13	41	86	186	470
MgO	-48	-44	-35	-26	-18	-14	-51	-40	-32	36	-95	-12.3
MnO	37	137	137	229	50	30	727	35	77	204	346	1220
CaO	-3.4	10.6	-1.7	23	-28	-41	-39	-39	-29	-7.8	-46	9.7
Na_2O	22	75	48	14	-18	-29	-89	-17	-22	-35	-92	-69
K_2O	9.9	-13	4.4	-2.7	-5.6	-23	-41	6.8	-1.8	-37	-39	-57
P_2O_5	2.9	7.1	1.4	2.7	6.3	-2.1	5.1	-4.2	5.9	7.1	-10.6	72
CO_2	312	285	103	6064	801	292	18	-100	324	-100	-100	2657
S	3449	1573	661	40458	16508	1859	15500	6542	8374	863	3162	17646
F	45	-35	-0.3	12.5	17.7	33	3.5	-10	31	70	57	20
Cl	-49	50	-48	5	-81	-62	-46	-64	-82	-24	10.5	-71
Ba	-2.8	-36	-12	-41	-31	-65	-56	-4	-33	-69	-71	-69
Rb	19	9.2	25		3.9	-2.1	-65	17	5	-14	-3.8	-97
Sr	23	36	28	-70	-37	-40	-39	-43	-53	-36	-46	-24
Zr	-4.7	1.4	-2.3	-8.7	4.3	-2.1	-43	1.4	-1.9	5.2	-0.7	-42
Y	19.5	21	18	15	16	10.6	10.6	14	30	21	6.7	-5.5
Nb	-73	-3.9	-73		6.7	8.3	-19	17	-5.2	22.8	17.6	-27
Be	-21	-8.2	-17.9	-6.1	-8.8	11.9	-32	-8.2	-9.2	6.2	15	-59
Cu	291	244	123	2859	508	135	4627	143	366	83	293	30567
Pb	-36	141	-37	1518	386	188	28706	14	317	305	325	36511
Zn	-3.1	76	76	722	275	170	1955	7.3	207	370	2879	32360
As	-96	-70	-57	-30	64	-38	857	7.4	124	144	-49	567
Bi	414	103	1.4	1749	462	95	727	1.4	112	1726	793	761
Sb	-66	384	-21	2119	275	118	3432	159	218	125	1668	1967
Cr	33	19	25	60	39	21	-65	74	18	25	31	113
Ni	-14	69	-15	516	-6.2	80	136	-32	41	69	64	216
Co	2.9	1.4	-8.7	307	24	-2.1	125	1.4	16.6	11.6	-10.6	555
V	-2.4	1.4	-1.2	4.3	6.8	10.5	-39	-3.8	3.2	1.4	5.4	50.2
Sc	-1.5	-1.8	-2.9	6.2	1.8	4.2	51	-2.9	1.4	0.3	4.6	47
La	5.0	7.8	-4.9	5.3	12.6	2.0	-11.4	-7.0	8.1	-4.9	2.4	4.1
Ce	19.6	29.7	10.9	25	31	13	1.7	10.9	23	12	25	36
Pr	-10.8	-19	-26	-18	-10	-21	-33	-26	-15	-26	-23	-23
Nd	23	19	6	20	29	15	-2.0	6.0	19	8.8	18	18
Sm	-6.5	-8.7	-18	-7.0	-3.8	-13	-26	-23	-13	-19	-10.6	-12
Eu	-36	-37	-42	-18	-30	-35	187	-37	-19	-28	-28	138
Gd	35	33	25	23	21	12	-2	10.8	21	15	29	29
Tb	10.8	1.4	-6.3	14	13	-2.0	-9.1	1.4	5.9	1.4	3.1	-11.2
Dy	22.5	21	15	25	23	14	7.8	19	26	22	10.4	-1.2
Ho	26.6	17	9.2	33	21	13	18	25	30	25	10	-4
Er	17	16	13	20	16	8.8	18	24	27	24	6.7	0.5
Tm	1.3	-7.8	-10.9	2.7	-2.8	-5.0	2.1	9.1	12	9.1	-9.3	-14
Yb	18	7.2	7.2	23	19	9	21	19	18	19	0.4	3.4
Lu	-6.8	-16	-14	0.2	-8.5	-11	1.6	-6.5	-7.3	-8.1	-13	-11
CF	1.03	1.01	1.01	1.23	1.13	0.98	1.18	1.01	1.06	1.01	0.89	1.72

* Notes: A correction factor $(CF = C^O_{Al2O3}/C^A_{Al2O3})$ was applied to the data displayed in Table 3 to compensate for mass changes resulting from alteration. The difference between mass-corrected data and least-altered sample was then ratioed to the least-altered sample and expressed as a percentage gain or loss of components. Sample 012 was used as the least-altered sample.

quartz assemblage, Woodland & Walther (1987) determined that Al solubility is prograde with temperature and pressure, but at 450°C and 1 kbar (100 MPa), the Al solubility is about 12 ppm ($10^{-3.4}$ molal). Its solubility relative to its abundance in the host rocks is critical. For example, a ratio of approximately 9 × 10^{-5} (Al_{aq}/Al_{rock}) in comparison to 3 × 10^{-3} (Si_{aq}/Si_{rock}) can be calculated using the data of Woodland & Walther (1987). In a detailed study of the surface samples around the Brunswick No. 6 deposit, Pearce (1963) normalized elements to Al_2O_3, as he considered Al to be immobile. The population variance of Al_2O_3 was compared with other high-field-strength elements (HFSE) traditionally considered immobile (Winchester & Floyd 1977, Davies et al. 1979, Pearce et al. 1984, MacLean 1990). The HFSE contents of these rocks is considerably more coherent than inferred by Finlow-Bates & Stumpfl (1981) in a regional study that included felsic volcanic and volcaniclastic rocks of the Bathurst Mining Camp. Nonetheless, the sample variances of the HFSE are greater than for Al_2O_3, consistent with variations in crystal/matrix ratio (Fig. 7).

The Al_2O_3 content of the least-altered rock (C^O_{Al2O3}) is compared to that in the altered equivalent (C^A_{Al2O3}) and corrected for the change in specific gravities between the altered rock (ρ^A) and least-

altered rock (ρ^O) to calculate the volume factor (f_v) (eq. 2). The volume factor (f_v) is:

$$f_v = C^O_{Al2O3}/C^A_{Al2O3} * (\rho^O/\rho^A) \qquad [2]$$

In order to calculate real mass-change ratio ($\Delta C_i/C^O_i$) for the rock (Grant 1986; eq. 3),

$$(\Delta C_i/C^O_i) = [(f_v)(\rho^A/\rho^O)(C^A_i/C^O_i) - 1] \qquad [3]$$

substituting equation 2 into 3,

$$(\Delta C_i/C^O_i) = (C^O_{Al2O3}/C^A_{Al2O3})(C^A_i/C^O_i) - 1 \qquad [4]$$

The isocon slope is used as a correction factor to adjust for the apparent change in concentration (expressed as a percent) between the altered rock (C^A_i) and parent rock (C^O_i).

Major- and trace-element systematics

After metamorphic dehydration of the altered protolith, the alteration of the QFAS to QAS is, for the most part, an isovolumetric process (i.e. $f_v \approx 1$) except for sample 006 ($f_v = 0.85$), which has an apparent reduction of 15% in volume. SiO_2 is relatively homogeneous, and MgO is quite variable across the sample profiles (Figs. 8A, B, Tables 3, 4). Na_2O increases noticeably within the transition zone [Q(F)AS] on one profile between the QFAS and QAS, reflecting albitization of the alkali feldspar. The partial hydrolysis of feldspar in the QFAS to form an assemblage of albite, sericite, and quartz [Q(F)AS] and further hydrolysis to chlorite and sericite (QAS) are coincident with a decrease in Na_2O, K_2O, CaO, and Ba (Figs. 8A, B). This is also probably responsible for a decrease in Sr and Rb (Figs. 8C, D). There is a pronounced enrichment of FeO_T and MnO (Figs. 8A, B), as well as H_2O in QAS relative to QFAS, reflecting the increased abundance of sericite and chlorite in the QAS. Although there is petrographic evidence of silicification of feldspar, the SiO_2 content is relatively unchanged, suggesting that either there is only local redistribution of silica as a result of hydrolysis reactions affecting the feldspar, or the degree of silicification near the outer margins of the feeder pipe is minor. Alternatively, the superimposed effects of silica leaching and enrichment obscure the path of alteration of the rock. The base metals increase in concentration in the more altered rocks as the ore zone is approached (Figs. 8C, D). This coincides with marked increases in CO_2 and S, which occur in sulfide and carbonate disseminations and veins, respectively. The F and Cl contents are irregular, directly reflecting variations in the content of sericite in the rock. The similarity of elemental variations between the two sample profiles indicates a common process and is consistent with previous interpretation of alteration effects around the Brunswick No. 12 deposit (Goodfellow 1975a, b, Luff et al. 1992).
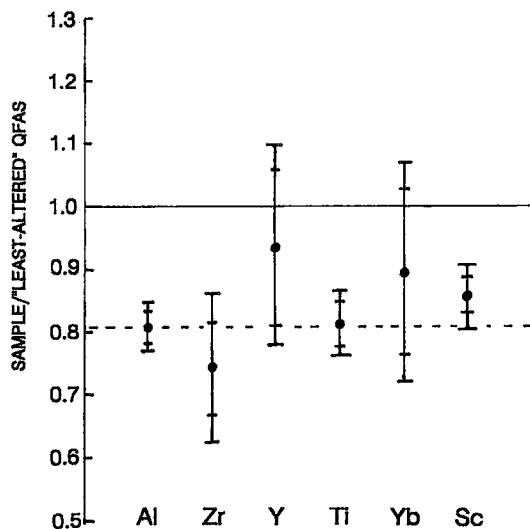
FIG. 7. Calculation of inverse volume factor ($1/f_v$) for sample 012 (least altered) and sample 153 using Al as the immobile element because of crystal-matrix heterogeneity in these felsic pyroclastic rocks and comparison with several other elements that are considered immobile. Error bars represent a 95% confidence interval based on the sample variance for QFAS [calculated from the data of McCutcheon (1990) and Lentz & Goodfellow (1992b)].
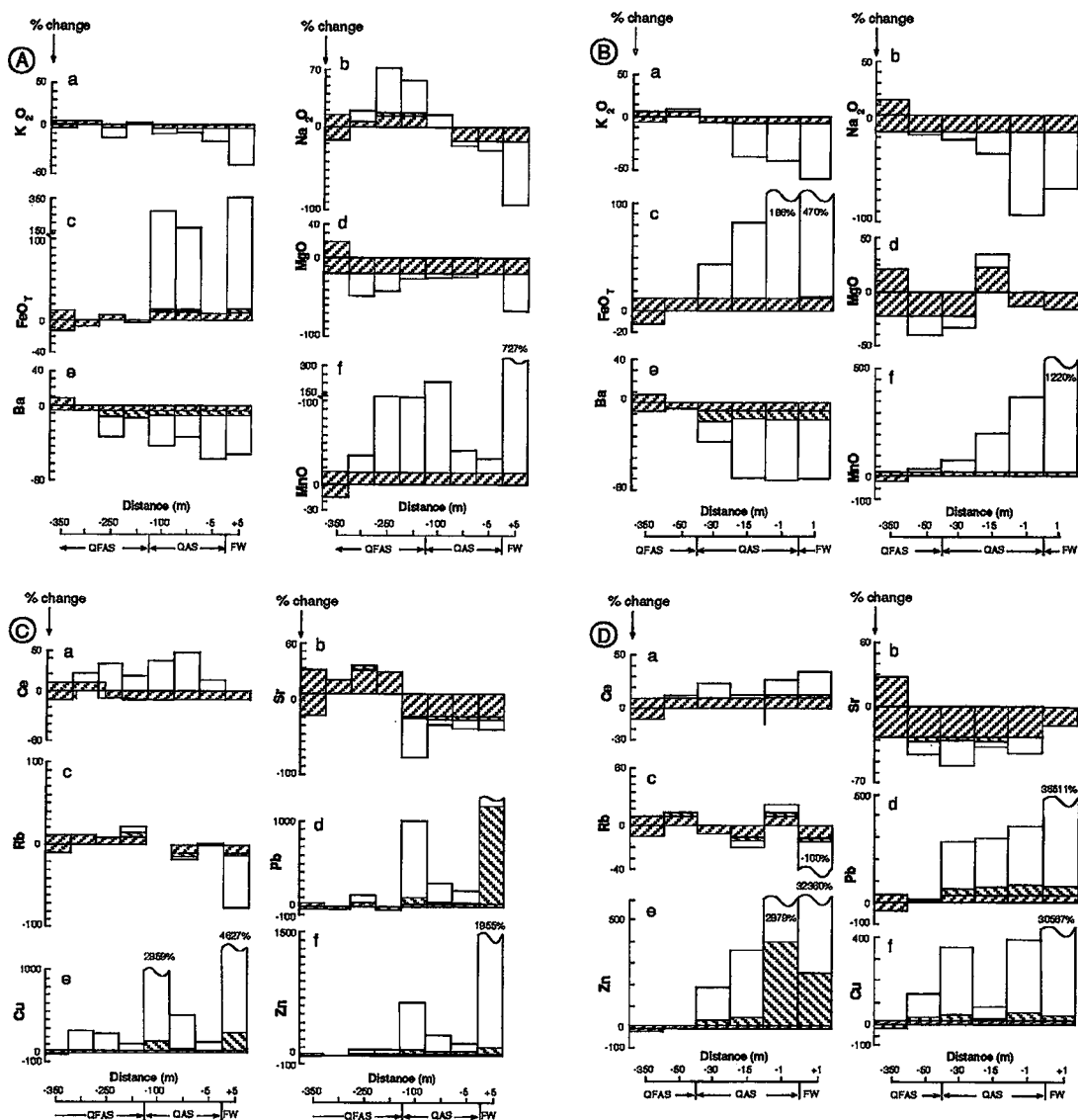
FIG. 8. Major- and trace-element mass-balance profiles from the least-altered crystal-rich tuff (QFAS) to the altered crystal-rich tuff (QAS) and footwall sedimentary rock (FW). These samples are normalized to the composition in the least-altered QFAS (LPA–012) after a correction factor (CF) is applied (see text for discussion). Cross-hatched bars /// represent a 95% confidence interval for sample variance of QFAS [calculated from the data of McCutcheon (1990) and Lentz & Goodfellow (1992b)]. The cross-hatched bars \\\ represent analytical error for the element. A) Major- and minor-element compositional profile from 50 m west of No. 3 shaft (LPA–150) to the footwall sedimentary rocks (LPA–156) on the 850-m level. B) Major- and minor-element compositional profile from 50 m east of QAS – footwall sedimentary rock contact to the footwall sedimentary rock on the 750-m level. C) Minor- and trace-element compositional profile from 50 m west of No. 3 shaft (LPA–150) to the footwall sedimentary rocks (LPA–156) on the 850-m level. D) Minor and trace-element compositional profile from 50 m east of QAS – footwall sedimentary rock contact to the footwall sedimentary rock on the 750-m level.

Lentz & Goodfellow (1992b) calculated average compositions of QFAS and QAS from the Brunswick No. 6 deposit (*cf.* McCutcheon 1990), which have

been used to qualitatively assess the overall effects of alteration. At the Brunswick No. 6 deposit, however, the QFAS and QAS do not represent a simple transi-
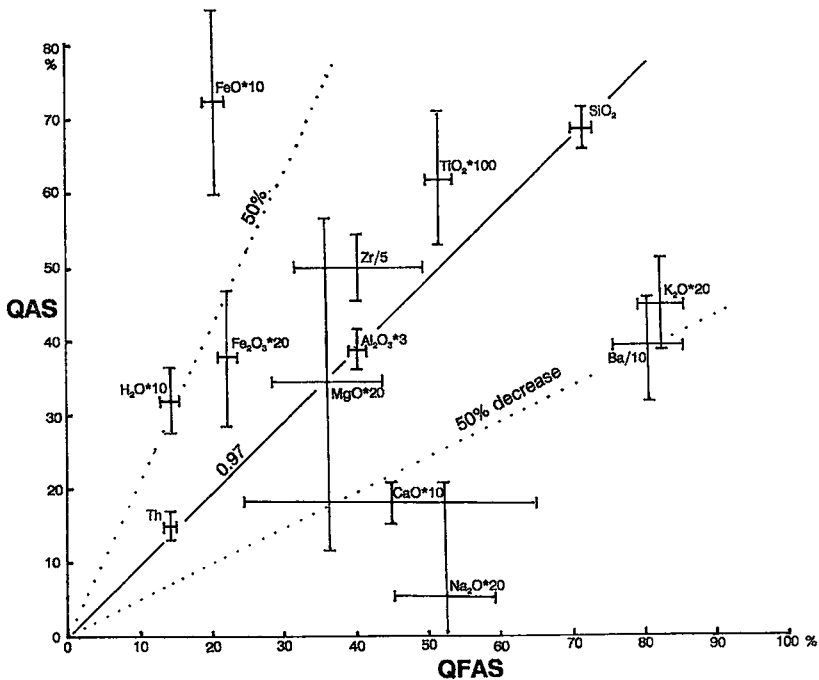
FIG. 9. Graphical mass-balance (isocon) diagram (Grant 1986) comparing the average
    composition of QAS with the average QFAS at the Brunswick No. 6 deposit using
    data from McCutcheon (1990), with the calculated 95% confidence intervals for those
    data. If Al_2O_3 is considered immobile, the volume factor (f_v) is 1.03, indicating no
    significant volume change. Note again that the Al_2O_3 variance is considerably smaller
    than for some of the other immobile species (Zr and TiO_2), possibly because of natur-
    al variation in the crystal/matrix ratio.

tion from one to the other, and the QAS unit is
intensely strained. The large variation in the crystal–
matrix ratio and intercalations of QAS with very fine-
grained sediment suggest sedimentary reworking of
the original crystal-rich pyroclastic unit (McCutcheon
1990). The high proportion of matrix to crystals in
portions of the QAS compared to the QFAS may
account for the apparently higher trace-element con-
tents, locally. Also, there are several shear-zones in
the footwall stratigraphy, as well as between the
QFAS and QAS (Pearce 1963), such that only general
conclusions can be made. The QAS unit, situated
stratigraphically beneath the ore, is significantly
enriched in FeO, Fe_2O_3, and H_2O, and depleted in
Na_2O, CaO, K_2O, and Ba, compared to the QFAS
(Fig. 9). SiO_2 content remains relatively unchanged,
although silica has definitely been redistributed during
hydrolysis of feldspar. Levels of MgO are highly vari-
able. These features reflect the intensity of sericitic
and chloritic alteration of the QFAS, as previously
noted by Pearce (1963). Within the Bathurst Camp,
similar geochemical features have been noted in the
altered footwall volcaniclastic rocks at the Key

Anacon massive sulfide deposit (Wahl 1978).

Rare-earth-element systematics

The chondrite-normalized *REE* contents of the
least-altered QFAS (Fig. 10) are similar and slightly
higher than the *REE* contents of other QFAS samples
from the Bathurst Camp (*cf.* Lentz & Goodfellow
1992b). The least-altered QFAS has a less pronounced
negative Eu anomaly than more altered samples, even
though concentrations of the trivalent *REE* are higher
in abundance. This attests to the minimal alteration of
this sample of QFAS (Fig. 10). The least-altered
QFAS was used to normalize the *REE* contents for the
remaining sample profiles, in order to observe the
REE variation with respect to the protolith (Figs. 11A,
B). As with the major- and trace-element data, the
REE have been corrected for mass change, in order to
identify slight variations in the *REE* abundances due to
alteration. The two horizontal lines represent the aver-
age variance (10%) of the sample population from
McCutcheon (1990) that may be due to variation in
the crystal/matrix ratio in the QFAS (Figs. 11, 12A,
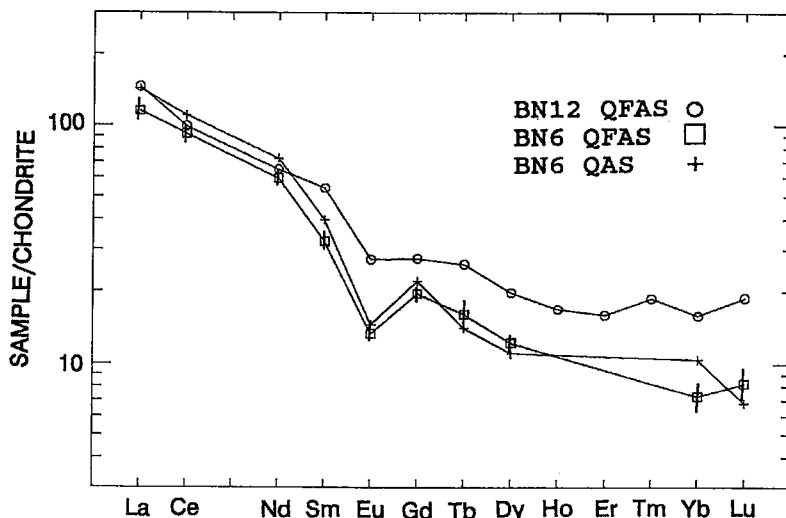
FIG. 10. Chondrite-normalized rare-earth element plot (Anders & Ebihara 1982) of least-altered crystal-rich tuff (QFAS, 012, this study) and Brunswick No. 6 least-altered crystal-rich tuff (QFAS) and altered crystal-rich tuff (QAS) (McCutcheon 1990).

B). Element variation within these limits is considered statistically insignificant. In general, the trivalent *REE* have remained relatively immobile, even in the moderately altered QAS. The light-rare-earth elements (*LREE*), in particular La, Ce, and Nd, have increased slightly in the altered rocks, with the possible exception of sample 156. The concentration of divalent Eu is lower in the two sample profiles relative to the "least-altered" QFAS, presumably owing to alteration of primary feldspar. Interestingly, however, the most altered QAS samples have the highest Eu contents in the two altered suites, reflecting the fixation of some of the mobilized Eu in the altered rocks, probably in carbonates. This may also account for the strong enrichment of Eu in the footwall sedimentary rocks. As previously described, the heavy-rare-earth elements (*HREE*) are relatively immobile within the altered rocks (Figs. 7, 11A, B). Although not described in detail in this study, the *HREE* systematics are potentially useful in chemostratigraphic analysis along the Brunswick Belt (cf. Lentz & Goodfellow 1992b). The average *REE* and trace-element contents were calculated for the QFAS and QAS (cf. Lentz & Goodfellow 1992b) from the footwall rocks of the Brunswick No. 6 deposit (McCutcheon 1990). On average, the QAS is enriched 20% in *LREE* (Al-normalized), which is slightly greater than the 10% variance described for the least-altered QFAS (95% confidence interval, Fig. 10). However, caution must be used, as Zr also is enriched by this order and was probably not enriched in the hydrothermal fluid. Europium is only slightly enriched in the altered QAS

compared to the parent QFAS. The *HREE* seem to be depleted by approximately 10% (not statistically significant) in the QAS (Fig. 11). Al-normalized data indicate that there is an average 20 ppm La enrichment in the silica–sulfide stringer mineralization, which has significant addition in volume (*i.e.*, >100%), whereas Yb seems to have been immobile (Lentz & Goodfellow 1993b).

The enrichment of *LREE* and Eu in the massive sulfides (Graf 1977) and associated Algoma-type iron formation (Graf 1978) along the Brunswick Belt indicates selective leaching of these components, probably as chloride complexes, from the underlying zone of hydrothermal reaction and their subsequent deposition within the upper parts of the hydrothermal vent complex and on the seafloor. This is consistent with major, trace, and *REE* mobility identified by mass-balance calculations of hydrothermally altered, footwall felsic volcanic rocks in other sulfide deposits (*e.g.*, Campbell *et al.* 1984, Bence & Taylor 1985, MacLean & Kranidiotis 1987, MacLean 1988, Barrett *et al.* 1991, de Groot & Baker 1992). Theoretical *REE*–ligand speciation (Wood 1990) and calculations of monazite solubility (Wood & Williams-Jones, in press) suggest that *LREE* elements are very low but more soluble than *HREE* as chloride complexes, although these preliminary calculations were based on salinities near those of seawater. Sverjensky (1984) and Wood (1990) showed that Eu would be divalent under the P, T, and oxygen fugacity conditions occurring in this vent complex. The inflection in the *REE* diagram at Yb may be analytical or possibly an indication of the
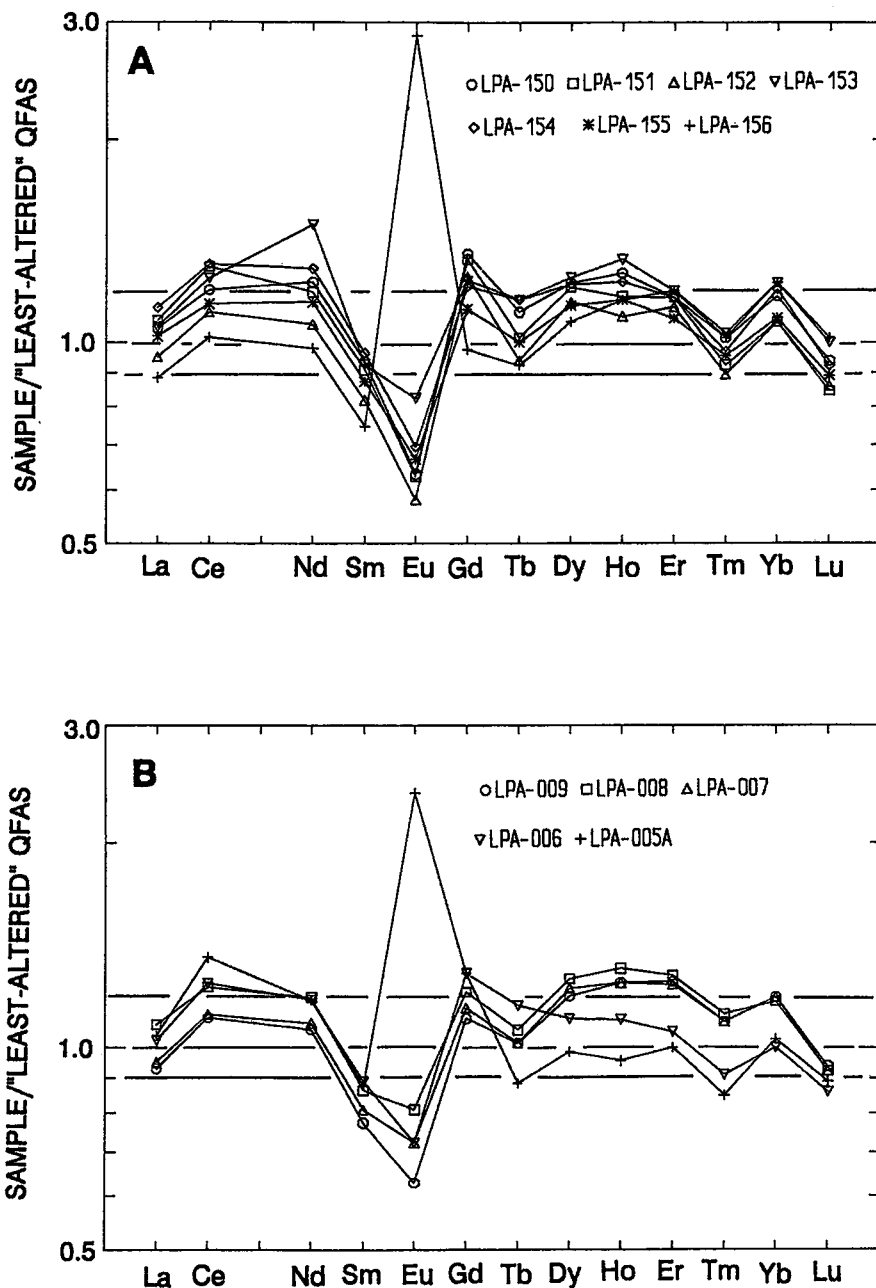
FIG. 11. "Least-altered" QFAS-normalized (LPA–012) distributions of the *REE* for the 850-m level (A) and the 750-m level (B) profiles. The horizontal lines at 1.1 and 0.9 represent the average variance (±10%) for the QFAS from the Brunswick No. 6 deposit area (see Fig. 10); therefore, variation within these limits cannot be considered significant enrichments or depletions with respect to the least-altered sample (LPA–012). Note that the footwall sedimentary rocks (FW) have significantly different distributions of *REE* compared to the crystal-rich tuffs (QFAS, QAS), which may be a function of sedimentary reworking.
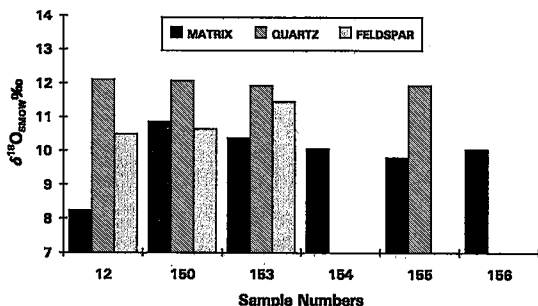
FIG. 12. Oxygen isotope compositions of paramorph after β quartz, feldspar phenocrysts, and matrix from the 850-m level section. The narrow distribution of $\delta^{18}O_{SMOW}$ value of the quartz reflects the homogeneity of the magma and a crustal source, whereas the matrix composition reflects most closely the fluid/rock (F/R) reactions associated with the alteration. The sample separates were analyzed using an Optima mass spectrometer at the University of Western Ontario, London, Ontario. Sample precision and accuracy are approximately 0.2‰.

divalent behavior of Yb at conditions of high temperatures and low oxygen fugacity, as predicted by Wood (1990).

OXYGEN ISOTOPE SYSTEMATICS

The overall distribution of the oxygen isotope values in matrix, quartz, and feldspar separates in samples from the 850-m level are illustrated in Figure 12. The quartz compositions are very uniform ($\delta^{18}O_{SMOW}$ between 11.92 and 12.11‰; Fig. 12) and indicative of primary igneous values. The microcline in samples 012 and 150 exhibits very minor alteration to mica, but the oxygen isotopic value remains relatively unchanged. However, the partially albitized and sericitized feldspar (sample 153) is enriched by about 1‰ over the pristine feldspar. The matrix of the least-altered rock (sample 012) has a low $\delta^{18}O$ value compared to the matrix composition of the adjacent sample (150). This probably reflects the primary glass composition, which is reasonable if compared to ^{18}O mineral – whole-rock distributions in felsic volcanic rocks, as reviewed by Taylor (1974), but requires further verification.

It is possible that the oxygen isotope composition of the matrix of a few of the least-altered QFAS samples increased slightly owing to weak albitization, as evident from the 22%, 75%, and 48% increase in Na in samples 150, 151, and 152, respectively. The fractionation factor for feldspar and water ($\Delta_{ab/w}$) is on the order of +6‰ at 300°C and +10‰ at 200°C (O'Neil & Taylor 1967), consistent with this trend. Munhá et al. (1980) indicated that K-feldspar alteration in felsic spilites occurs below 140°C, whereas albitization

occurs between 140° and 230°C. Therefore, feldspathization can occur over a considerable range in temperatures and water/rock ratios, thus producing overall increases in $\delta^{18}O$ of +4 to +6‰ over unaltered precursors, although an increase of 2.5‰ from the matrix of samples 012 to 150 suggests that albitization either occurred at higher temperatures or lower fluid/rock ratio. The decreasing $\delta^{18}O$ value of matrix samples 151 to 156 is coincident with an increase in the proportion of chlorite. The fractionation factor between micas and water is considerably lower than between feldspar and water ($\Delta_{musc-H2O}$ = +3‰ at 300°C and $\Delta_{chl-H2O}$ = 0 at 300°C: O'Neil & Taylor 1969, Wenner & Taylor 1971). Because these values are superimposed onto ^{18}O-enriched felsic volcanic rocks (QFAS), the differences in whole-rock oxygen isotopes may be mainly a function of the secondary mineral assemblage, i.e., albitization versus sericitization and chloritization (cf. Munhá et al. 1980, Bence & Taylor 1985, Taylor & South 1985).

HYDROTHERMAL REACTIONS

The least-altered QFAS exhibits variable degrees of alteration by seawater owing to devitrification of glass (variable MgO ± Na$_2$O). The presence of secondary (authigenic?) alkali feldspar (cf. Nelson 1983), as well as albite, indicates the aNa$^+$/aK$^+$ of seawater was modified as a result of hydrothermal exchange-reactions in the felsic pyroclastic sequence. The fixation of Mg(OH)$_{2\ aq}$ in clays is probably responsible for Mg enrichment and has been attributed to a pronounced decrease of pH of the fluid in felsic volcanic (Dickson 1977) and immature sedimentary rocks (Bischoff et al. 1981). The transition between QFAS and QAS is characterized by albite ± muscovite, Mg-rich chlorite, and sulfides pseudomorphically replacing K-feldspar. The partial alteration of alkali feldspar in the transition zone along the margin of the venting hydrothermal fluids is indicative of low fluid–rock ratios or fluid compositions that approached equilibrium with the rock. Commonly, these two factors are closely related. These assemblages are characteristic of weakly acidic to neutral pH conditions at aNa$^+$/aK$^+$ ≥ 2 (but less than seawater, Fig. 13). The slight enrichment of Na, Fe, Mn, S, CO$_2$, base metals (± Mg, Ca) remote from the sulfide deposit is characteristic of the distal zone of alteration. Mass-balance calculations indicate that this is approximately an isovolumetric process, consistent with the pervasive nature of the alteration at or near lithostatic pressure. This zone of alteration may have formed by the interaction of the upwelling and laterally migrating hydrothermal fluid with the weakly altered crystal-rich tuffs and with cooler shallowly circulating seawater.

The reaction of the venting hydrothermal fluid with weakly altered felsic volcanic rocks is probably responsible for hydrolysis of primary and secondary
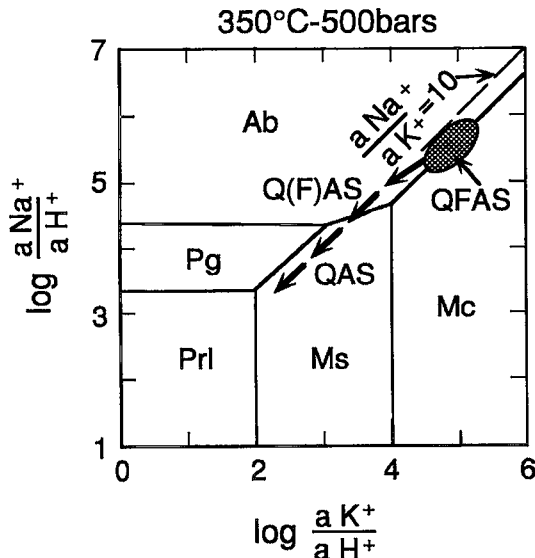
350°C-500bars

FIG. 13. Stability fields of mineals in the system $HCl - H_2O - K_2O - Na_2O - SiO_2 - Al_2O_3$ at 350°C and 500 bars (50 MPa) at quartz saturation (cf. Bowers et al. 1984). The albite–muscovite boundary occurs at a pH of 3.9 if NaCl = 3 M and KCl = 0.5 M. This diagram illustrates the relative stabilities of the alteration assemblages. The stability of albite is principally a function of aNa^+/aK^+. QFAS: least-altered crystal-rich tuff, Q(F)AS: weakly altered crystal-rich tuff, QAS: moderately altered crystal-rich tuff. Mineral abbreviations after Kretz (1983).

feldspars to phengite, Mg–Fe-bearing chlorite, and quartz (eq. 5, Fig. 13). Equation 5 represents the hydrolysis of albite to sericite at conditions of moderately acidic pH conditions (pH approximately 3.9), at salinities (NaCl = 3 m and KCl = 0.5 m) and temperatures typical of venting hydrothermal fluids (350°C, cf. Bowers et al. 1984).

$$3 NaAlSi_3O_8 + K^+_{aq} + 2 H^+_{aq} \rightarrow$$
$$\text{albite} \rightarrow$$
$$KAl_3Si_3O_{10}(OH)_2 + 6 SiO_2 + 3 Na^+_{aq} \qquad [5]$$
$$\text{sericite} \qquad \text{quartz}$$
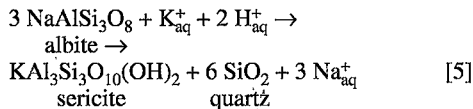
300.8 cm³/mole → 140.8 cm³/mole + 136.1 cm³/mole.

The SiO_2 portion of equation 5 is probably quartz, although some silica was probably transported as a $Si(OH)_4$ complex. If the reaction (eq. 5) involves the complete hydrolysis of feldspar (proceeds to the right), the hydrothermal fluid is moderately acidic (pH ≤ 3.9) and is no longer buffered by the presence of feldspar provided that the aNa^+/aK^+ remains unchanged. The increase in Fe/(Fe+Mg) of chlorite and phengitic sericite toward the main hydrothermal conduit (Fig. 13) is indicative of higher aFe^{2+}/aMg^{2+} at a

moderately acidic pH. The mineralogical enrichment in Fe relative to Mg also coincides with a modal increase in the content of chlorite that involves a protolysis reaction.

$$K_2Fe^{2+}Al_3Si_7AlO_{20}(OH)_4 + 9 FeCl_{2\,aq} + 16 H_2O \rightarrow$$
$$\text{phengite}$$
$$Fe^{2+}_{10}Al_2Si_6Al_2O_{20}(OH)_{16} + H_4SiO_{4aq} + \qquad [6]$$
$$\text{Fe-rich chlorite}$$
$$2 KCl_{aq} + 16 HCl$$
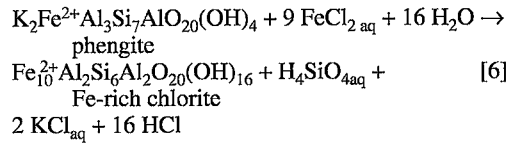
The end-member reaction (eq. 6) has been formulated assuming Al immobility (i.e., it conserves aluminum), which illustrates the relative behaviors of mobile components. This reaction shifts to the right owing to high activities of $FeCl_2$ in the discharging fluid. This reaction also may be responsible for the liberation and redistribution of silica in the altered products. Silica leaching is evident in the most intensely altered portions of the deposit, but less so with the alteration of the QFAS to QAS. An increase in Fe/(Fe+Mg) coincides with the increased Al content of mica that formed at the expense of silica, and these chemical changes should reflect the decrease in silica. The dissolution of silica should increase with temperature owing to the prograde solubility of quartz (cf. Fournier 1985). Intense silicification is evident in the upper parts of the hydrothermal feeder system and within the basal massive sulfide zone (Lentz & Goodfellow 1993a, b).

DISCUSSION

The quartz augen have previously been interpreted as relict phenocrysts in deformed and metamorphosed felsic pyroclastic rocks (Vernon & Flood 1977, Vernon 1986) or as porphyroblasts that formed during the greenschist-grade regional metamorphism associated with regional deformation (Hopwood 1976, 1977). The absence of feldspar in these rocks (QAS) also has been attributed to feldspar weathering and resedimentation (McCutcheon 1990, 1992). Within the vicinity of the Brunswick No. 6 and 12 deposits, the similar textures in the QAS and QFAS, and the proximity of the QAS to hydrothermal feeder zones related to exhalative massive sulfide deposits, led Goodfellow (1975a, b), Juras (1981), Nelson (1983), and Luff et al. (1992) to interpret the QAS as a product of hydrothermal alteration. The chlorite- and sericite-bearing QAS, which forms part of the footwall sequence at the Brunswick No. 12 deposit, has been interpreted as a product of hydrothermal alteration of QFAS related to the formation of the massive sulfide deposits or to seafloor alteration (Goodfellow 1975a, b, Juras 1981, Nelson 1983, Lentz & Goodfellow 1992a, Luff et al. 1992). The similarity of textures, presence of mica–quartz pseudomorphs after alkali feldspar, and homogeneously distributed, matrix-supported, cataclastic to euhedral quartz, the grada-

tional transition from QFAS to QAS over tens to hundreds of meters, and the absence of grading or bedding features do not favor an epiclastic origin for the bulk of the QAS at the mine. Therefore, it is likely that the QAS is an *in situ* altered medium- to coarse-grained variety of the coarse-grained quartz–feldspar crystal tuff (QFAS). Furthermore, the presence of mica–quartz pseudomorphs after feldspar does not represent porphyroblastic growth of quartz during regional metamorphism or deformed volcanic quartz, although "vitreous" volcanic quartz is present.

In both sections sampled at the Brunswick No. 12 deposit, the footwall sedimentary rocks exhibit the effects of alteration more than the adjacent QAS, although there is a continuum across the contact. The alteration in the footwall sedimentary rocks is heterogeneous. Sample 005A of footwall sedimentary rock contains abundant fine-grained "vitreous" quartz and is moderately chloritized and weakly mineralized (Table 3). Sample 005B, on the other hand, is intensely chloritized and mineralized, although moderately altered sericite–chlorite footwall sedimentary rocks are the most prevalent just above the QAS. The tuffaceous footwall sediments seem to be more susceptible to hydrothermal alteration, possibly because of the differences in porosity and permeability across the contact if they remained semiconsolidated at the time of mineralization. Alternatively, a high proportion of devitrified glass may have enhanced the reactivity of the unit, in an analogous way to the case of altered sediments in sedimented hydrothermally active rifts (Goodfellow & Blaise 1988). This could also explain the extensive lateral distribution of chloritic alteration within the footwall sedimentary rocks directly beneath the massive sulfide, as described by Goodfellow (1975a, b) and Luff *et al.* (1992).

Although the mineralizing hydrothermal fluid responsible for the alteration was permeability-controlled, the slight decrease in volume ($f_v \leqslant 1$) in the weakly to moderately altered QAS is consistent with geostatic pressures approaching lithostatic (*i.e.*, $P(H_2O) \leqslant P_{lith}$) compared to the sulfide-stringer zone (Lentz & Goodfellow 1993b). These conditions promote a more pervasive style of alteration and tend to produce a greater proportion of disseminated mineralization than is observed in the footwall sequence. The disseminated style of mineralization and the small changes in volume indicate that the profiles sampled in this study probably represent the margin of the fluid–discharge conduit. Chlorite, quartz, and sulfide veins, and coarse network breccias (stringer-sulfide veins) are more common in the core of the hydrothermal discharge system (Lentz & Goodfellow 1993a). The feeder pipe itself may be interpreted as evidence for the existence of a synvolcanic fault that focussed fluid flow to the seafloor (Luff *et al.* 1992, Lentz & Goodfellow 1993a).

The alteration of alkali feldspar phenocrysts in crystal-rich felsic pyroclastic rocks is a characteristic feature of alteration zones associated with the Brunswick No. 12 massive sulfide deposit. The hydrothermal alteration of the crystal-rich pyroclastic rock enables its use as an exploration guide for the identification of paleohydrothermal zones of fluid upflow that may have formed sulfide deposits. The occurrence of augen-shaped seriate aggregates of quartz and mica with coarse-grained, subrounded to angular "vitreous" quartz is interpreted to have formed by seafloor hydrothermal alteration of alkali feldspar. In a similar study, Frater (1983) described petrographically three "generations" of quartz-eye schists at the Golden Grove massive sulfide Cu–Zn deposit, in Australia: 1) volcanic quartz, 2) metasomatic replacement of feldspar, and 3) diagenetic or metamorphic overgrowths and infillings. The metasomatic replacement of feldspar is related to the hydrothermal alteration by mineralizing fluids, as was found in this study. Feldspar alteration in volcanic rocks underlying massive sulfide deposits has long been recognized (Roberts & Reardon 1978, Riverin & Hodgson 1980, Wynne & Strong 1984, Kranidiotis & MacLean 1987). The intensity of penetrative deformation is considerably greater in the Bathurst Camp, which complicates the identification and characterization of alteration with respect to premetamorphic assemblages of hydrothermal minerals. For instance, the occurrence of albite, phengite, and chlorite is also typical of greenschist-grade assemblages. However, the examination of relict textures in low-strain domains and the paragenesis of these minerals have helped to differentiate between products of hydrothermal alteration and products of metamorphism.

CONCLUSIONS

1) The QAS unit transgresses the stratigraphy and primary S_1 and S_2 fabrics in the upper portions of the mine, indicating that it is a not a sedimentary unit or related to deformation.

2) The pseudomorphic replacement of coarse-grained alkali feldspar phenocrysts by granoblastic quartz, albite, and mica has resulted from the hydrothermal alteration of the coarse-grained crystal-rich tuff (QFAS). Secondary albite, phengitic sericite, and Mg-rich chlorite have formed in the transition zone [Q(F)AS] between the least-altered (QFAS) and altered (QAS) crystal-rich tuff. Within the QAS, the quartz-rich ($\pm$ phengite, albite, chlorite) pseudomorphs (augen) with disseminated sulfides is characteristic of the alteration associated with the massive sulfide deposits hosted within volcanic sequences.

3) Phenocrysts of "vitreous" volcanic quartz occur with the mica-bearing milky quartz augen in the Q(F)AS and QAS.

4) The greater proportion of mica in the QAS may explain why there is a well-developed $S_1 S_2$ composite

fabric and numerous strain-related features in this unit. The volcanic quartz deforms cataclastically, whereas the quartz–mica pseudomorphs behave in a more ductile fashion.

5 The mineral compositions reflect, quite closely, the major-element changes within the rocks.

6) On the basis of mass-balance calculations, the hydrothermal alteration on the margins of the feeder zone is responsible for the formation of the Q(F)AS, which is characterized by slight enrichments of Na, Fe, Mn, S, CO_2 and base metals, and erratic Mg and Ca contents. The moderately altered QAS is enriched, with respect to the QFAS (parent), in Fe, Mn, S, CO_2, and base metals, and depleted in Na, K, Ca, Ba, Rb and Sr. SiO_2 does not vary significantly. These effects of alteration are more pronounced in the footwall sedimentary rocks just above the QAS contact.

7) Alteration features described above for the Brunswick No. 12 deposit also are recognized in the rocks underlying the Brunswick No. 6 deposit and along the Brunswick belt.

8) The hydrolysis of feldspar and the replacement of sericite by Fe-rich chlorite toward the more altered QAS and footwall sedimentary rocks indicate moderately acidic and high aFe^{2+}/aMg^{2+} conditions in the reacting hydrothermal fluids.

9) Although some of the evidence is equivocal, the QAS that usually overlies the QFAS was probably formed by hydrothermal alteration of QFAS near the zone of hydrothermal discharge.

REFERENCES

ANDERS, E. & EBIHARA, M. (1982): Solar-system abundances of the elements. Geochim. Cosmochim. Acta 46, 2363-2380.

BARRETT, T.J., MACLEAN, W.H., CATTALANI, S., HOY, L. & RIVERIN, G. (1991): Massive sulfide deposits of the Noranda area, Quebec. III. The Ansil mine. Can. J. Earth. Sci. 28, 1699-1730.

BATTEY, M.H. (1955): Alkali metasomatism and the petrology of some keratophyres. Geol. Mag. 92, 104-126.

BENCE, A.E. & TAYLOR, B.E. (1985): Rare earth element systematics of West Shasta metavolcanic rocks: petrogenesis and hydrothermal alteration. Econ. Geol. 80, 2164-2176.

BISCHOFF, J.L., RADTKE, A.S. & ROSENBAUER, R.J. (1981): Hydrothermal alteration of graywacke by brine and seawater. Roles of alteration and chloride complexing on metal solubilization at 200° and 350°C. Econ. Geol. 76, 659-676.

BOWERS, T.S., JACKSON, K.J. & HELGESON, H.C. (1984): Equilibrium Activity Diagrams for Coexisting Minerals and Aqueous Species at Pressures and Temperatures to 5 kb and 600°C. Springer-Verlag, Berlin.

BRINDLEY, G.W. & YOUELL, R.F. (1953): Ferrous chamosite and ferric chamosite. Mineral. Mag. 30, 57-70.

CAMERON, B.I., HANNINGTON, M.D., BRISBIN, D.I. & KOOPMAN, E.R. (1993): Preliminary mineral chemical studies of phyllosilicates in host rocks of the Kidd Creek massive sulphide deposit, Timmins, Ontario. Geol. Surv. Can., Pap. 93-1E, 157-164.

CAMPBELL, I.H., LESHER, C.M., COAD, P., FRANKLIN, J.M., GORTON, M.P., & THURSTON, P.C. (1984): Rare-earth element mobility in alteration pipes below massive Cu–Zn sulfide deposits. Chem. Geol. 45, 181-202.

CATHELINEAU, M. & NIEVA, D. (1985): A chlorite solid solution geothermometer: the Los Azufres (Mexico) geothermal system. Contrib. Mineral. Petrol. 91, 235-244.

DAVIES, J.F., GRANT, R.W.E. & WHITEHEAD, R.E.S. (1979): Immobile trace elements and Archean volcanic stratigraphy in the Timmins mining area, Ontario. Can. J. Earth. Sci. 16, 305-311.

DE GROOT, P.A. & BAKER, J.A. (1992): High element mobility in 1.9 – 1.86 Ga hydrothermal alteration zones, Bergslagen, central Sweden: relationships with exhalative Fe-ore mineralizations. Precambrian Res. 54, 109-130.

DEER, W.A., HOWIE, R.A. & ZUSSMAN, J. (1962): Rock-Forming Minerals. 3. Sheet Silicates. Longmans Canada Ltd., Toronto, Ontario.

DICKSON, F.W. (1977): The role of rhyolite–seawater reaction in the genesis of Kuroko ore deposits. In Proc. Second Int. Symp. on Water-Rock Interaction (Strasbourg). International Association of Geochemistry and Cosmochemistry IV, 181-190.

FINLOW-BATES, T. & STUMPFL, E.F. (1981): The behaviour of so-called immobile elements in hydrothermally altered rocks associated with volcanogenic submarine-exhalative ore deposits. Mineral. Deposita 16, 319-328.

FOURNIER, R.O. (1985): The behavior of silica in hydrothermal solutions. *In* Geology and Geochemistry of Epithermal Systems (B.R. Berger & P.M. Bethke, eds.). *Rev. Econ. Geol.* **2**, 45-61.

FRATER, K.M. (1983): Effects of metasomatism and development of quartz "eyes" in intrusive and extrusive rocks at Golden Grove Cu–Zn deposit, Western Australia. *Trans. Inst. Min. Metall. (sect. B)* **92**, B121-B131.

FYFFE, L.R. & SWINDEN, H.S. (1991): Paleotectonic setting of Cambro-Ordovician volcanic rocks in the Canadian Appalachians. *Geosci. Can.* **18**, 145-157.

GOODFELLOW, W.D. (1975a): Major and minor element halos in volcanic rocks at the Brunswick no. 12 sulphide deposit, N.B., Canada. *In* Geochemical Exploration 1974 (I.L. Elliot & W.K. Fletcher, eds.). Elsevier, Amsterdam (279-295).

———— (1975b): *Rock Geochemical Exploration and Ore Genesis at the Brunswick No. 12 Deposit*. Ph.D. thesis, Univ. New Brunswick, Fredericton, New Brunswick.

———— & BLAISE, B. (1988): Sulfide formation and hydrothermal alteration of hemipelagic sediment in Middle Valley, northern Juan de Fuca Ridge. *Can. Mineral.* **26**, 675-696.

GRAF, J.L., JR. (1977): Rare earth elements as hydrothermal tracers during the formation of massive sulfide deposits in volcanic rocks. *Econ. Geol.* **72**, 527-548.

———— (1978): Rare earth elements, iron formation and seawater. *Geochim. Cosmochim. Acta* **42**, 1845-1850.

GRANT, J.A. (1986): The isocon diagram – a simple solution to Gresens' equation for metasomatic alteration. *Econ. Geol.* **81**, 1976-1082.

GRESENS, R.L. (1967): Composition – volume relationships of metasomatism. *Chem. Geol.* **2**, 47-65.

HENDRY, D.A.F. (1981): Chlorites, phengites, and siderites from the Prince Lyell ore deposits, Tasmania, and the origin of the deposit. *Econ. Geol.* **76**, 285-303.

HEY, M.H. (1954): A new review of the chlorites. *Mineral. Mag.* **30**, 277-292.

HOPWOOD, T.P. (1976): "Quartz-eye"-bearing porphyroidal rocks and massive sulfide deposits – a reply. *Econ. Geol.* **71**, 589-612.

———— (1977): "Quartz-eye"-bearing porphyroidal rocks and massive sulfide deposits – a reply. *Econ. Geol.* **72**, 701-703.

HUGHES, C.J. (1973): Spilites, keratophyres, and the igneous spectrum. *Geol. Mag.* **109**, 513-527.

JAMBOR, J.L. (1979): Mineralogical evaluation of proximal–distal features in New Brunswick massive sulphide deposits. *Can. Mineral.* **17**, 649-664.

———— (1981): Mineralogy of the Caribou massive sulphide deposit, Bathurst area, New Brunswick. *Energy, Mines, and Resources Canada, CANMET Rep.* **81-8E**.

JURAS, S.J. (1981): *Alteration and Sulphide Mineralization in Footwall Felsic and Sedimentary Rocks, Brunswick No. 12 Deposit, Bathurst, New Brunswick, Canada*. M.Sc. thesis, Univ. New Brunswick, Fredericton, New Brunswick.

KRANIDIOTIS, P. & MACLEAN, W.H. (1987): Systematics of chlorite alteration at the Phelps Dodge massive sulfide deposit, Matagami, Quebec. *Econ. Geol.* **82**, 1898-1911.

KRETZ, R. (1959): Chemical study of garnet, biotite, and hornblende from gneisses of southwestern Quebec, with emphasis on distribution of elements in coexisting minerals. *J. Geol.* **67**, 371-402.

———— (1983): Symbols for rock-forming minerals. *Am. Mineral.* **68**, 277-279.

LEITCH, C.H.B. (1992): Mineral chemistry of selected silicates, carbonates, and sulphides in the Sullivan and North Star stratiform Zn–Pb deposits, British Columbia, and in district-scale altered and unaltered sediments. *Geol. Surv. Can., Pap.* **92-1E**, 83-93.

LE MAITRE, R.W. (1982): *Numerical Petrology*. Elsevier, New York.

LENTZ, D.R. & GOODFELLOW, W.D. (1992a): Re-evaluation of the petrology and depositional environment of felsic volcanic and related rocks in the vicinity of the Brunswick No. 12 massive sulphide deposit, Bathurst Mining Camp, New Brunswick. *Geol. Surv. Can., Pap.* **92-1E**, 333-342.

———— & ———— (1992b): Re-evaluation of the petrochemistry of felsic volcanic and volcaniclastic rocks near the Brunswick No. 6 and 12 massive sulphide deposits, Bathurst Mining Camp, New Brunswick. *Geol. Surv. Can., Pap.* **92-1E**, 343-350.

———— & ———— (1993a): Mineralogy and petrology of the stringer sulphide zone in the Discovery Hole at the Brunswick No. 12 massive sulphide deposit, Bathurst, New Brunswick. *Geol. Surv. Can. Pap.* **93-1E**, 249-258.

———— & ———— (1993b): Geochemistry of the stringer sulphide zone in the Discovery Hole at the Brunswick No. 12 massive sulphide deposit, Bathurst, New Brunswick. *Geol. Surv. Can., Pap.* **93-1E**, 259-269.

———— & VAN STAAL, C.R. (1992): Geological implications of post-ore and pre-deformation emplacement of the "felsic" dike at the Brunswick No. 12 deposit, Bathurst, New Brunswick. *Geol. Assoc. Can. – Mineral. Assoc. Can., Program Abstr.* **17**, A65.

LEWCZUK, L. (1990): Microprobe analyses of phyllosilicates, Bathurst Camp. *New Brunswick Research and Productivity Council, Rep.*

LOUDON, J.R. (1960): *The Origin of the Porphyry and Porphyry-Like Rocks of the Elbow, New Brunswick*. Ph.D. thesis, Univ. Toronto, Toronto, Ontario.

LUFF, W., GOODFELLOW, W.D. & JURAS, S. (1992): Evidence for a feeder pipe and associated alteration at the Brunswick No. 12 massive sulphide deposit. *Expl. Min. Geol.* **1**, 167-185.

MACLEAN, W.H. (1988): Rare earth element mobility at constant inter-*REE* ratios in the alteration zone at the Phelps Dodge massive sulphide deposit, Matagami, Quebec. *Mineral. Deposita* **23**, 231-238.

——— (1990): Mass change calculations in altered rock series. *Mineral. Deposita* **25**, 44-49.

——— & KRANIDIOTIS, P. (1987): Immobile elements as monitors of mass transfer in hydrothermal alteration: Phelps Dodge massive sulfide deposit, Matagami, Quebec. *Econ. Geol.* **82**, 951-962.

MASSONNE, H.-J. & SCHREYER, W. (1987): Phengite geobarometry based on the limiting assemblage with K-feldspar, phlogopite, and quartz. *Contrib. Mineral. Petrol.* **96**, 212-224.

MCCUTCHEON, S.R. (1990): Base-metal deposits of the Bathurst–Newcastle district. *In* Field guide to massive sulphide deposits in northern New Brunswick (L.R. Fyffe, ed.). Base Metal Symposium 1990, Minerals and Energy Division, Department of Natural Resources and Energy, New Brunswick (42-71).

——— (1992): Base-metal deposits of the Bathurst-Newcastle district: characteristics and depositional models. *Expl. Min. Geol.* **1**, 105-119.

MCLEOD, R.L. & STANTON, R.L. (1984): Phyllosilicates and associated minerals in some Paleozoic stratiform sulfide deposits of southeastern Australia. *Econ. Geol.* **79**, 1-22.

MUNHÁ, J., FYFE, W.S. & KERRICK, R. (1980): Adularia, the characteristic mineral of felsic spilites. *Contrib. Mineral. Petrol.* **75**, 15-19.

NELSON, G.A. (1983): *Alteration of Footwall Rocks at Brunswick No. 6 and Austin Brook Deposits, Bathurst, New Brunswick, Canada*. M.Sc. thesis, Univ. New Brunswick, Fredericton, New Brunswick.

O'NEIL, J.R. & TAYLOR, H.P., JR. (1967): The oxygen isotope and cation exchange chemistry of feldspars. *Am. Mineral.* **52**, 1414-1437.

——— & ——— (1969): Oxygen isotope equilibrium between muscovite and water. *J. Geophys. Res.* **74**, 6012-6022.

PEARCE, J.A., HARRIS, N.B.W. & TINDLE, A.G. (1984): Trace element discrimination diagrams for the tectonic interpretation of granitic rocks. *J. Petrol.* **25**, 956-983.

PEARCE, T.H. (1963): *The Petrochemistry and Petrology of the Quartz–Feldspar Porphyry, Bathurst, New Brunswick*. M.Sc. thesis, Univ. Western Ontario, London, Ontario.

RAMAMOHANA RAO, T. (1977): Distribution of elements between coexisting phengite and chlorite from the greenschist facies of the Tennant Creek area, central Australia. *Lithos* **10**, 103-112.

RIVERIN, G. & HODGSON, C.J. (1980): Wall-rock alteration at the Millenbach Cu–Zn mine, Noranda, Quebec. *Econ. Geol.* **75**, 424-444.

ROBERTS, R.G. & REARDON, E.J. (1978): Alteration and ore-forming processes at Mattagami Lake Mine, Quebec. *Can. J. Earth Sci.* **15**, 1-21.

SKINNER, R. (1974): Geology of Tetagouche Lakes, Bathurst, and Nepisiguit Falls map-areas, New Brunswick with emphasis on the Tetagouche Group. *Geol. Surv. Can., Mem.* **371**.

SLACK, J.F. & COAD, P.R. (1989): Multiple hydrothermal and metamorphic events in the Kidd Creek volcanogenic massive sulfide deposit, Timmins, Ontario: evidence from tourmalines and chlorites. *Can. J. Earth Sci.* **26**, 694-715.

———, JIANG, WEI-TEH, PEACOR, D.R. & OKITA, P.M. (1992): Hydrothermal and metamorphic berthierine from the Kidd Creek volcanogenic massive sulfide deposit, Timmins, Ontario. *Can. Mineral.* **30**, 1127-1142.

STARKEY, J. (1959): Chess-board albite from New Brunswick, Canada. *Geol. Mag.* **96**, 141-145.

SUTHERLAND, J.K. (1967): Chlorites of the Anaconda-Caribou deposit, New Brunswick. *New Brunswick Research and Productivity Council Report, Research Note* **8**.

SVERJENSKY, D.A. (1984): Europium redox equilibria in aqueous solution. *Earth Planet. Sci. Lett.* **67**, 70-78.

TAYLOR, B.E. & SOUTH, B.C. (1985): Regional stable isotope systematics of hydrothermal alteration and massive sulfide deposition in the West Shasta District, California. *Econ. Geol.* **80**, 2149-2163.

TAYLOR, H.P., JR. (1974): The application of oxygen and hydrogen isotopes studies to problems of hydrothermal alteration and ore deposition. *Econ. Geol.* **69**, 843-883.

VAN STAAL, C.R. (1985): *The Structure and Metamorphism of the Brunswick Mines Area, Bathurst, New Brunswick, Canada*. Ph.D. thesis, Univ. New Brunswick, Fredericton, New Brunswick.

——— (1987): Tectonic setting of the Tetagouche Group in northern New Brunswick: implications for plate tectonic models in the northern Appalachians. *Can. J. Earth. Sci.*, **24**, 1329-1351.

——— (1992): Geology and structure of the Brunswick Mines area (21-P5 e,f). *New Brunswick Dep. Nat. Resources, MR Open-File Map* **91-40f**.

——— & FYFFE, L.R. (1991): The New Brunswick Dunnage and Gander Zones. *In* The Appalachian/Caledonian

Orogen, Canada and Greenland (H. Williams, co-ordinator). *Decade of North American Geology, Vol.* **F-1** (in press).

————, ————, LANGTON, J.P. & McCUTCHEON, S.R. (1992): The Ordovician Tetagouche Group, Bathurst Camp, northern New Brunswick, Canada: history, tectonic setting and distribution of massive sulphide deposits. *Expl. Min. Geol.* **1**, 93-103.

————, RAVENHURST, C.E., WINCHESTER, J.A., RODDICK, J.C. & LANGTON, J.P. (1990): Post-Taconic blueschist suture in the northern Appalachians of northern New Brunswick, Canada. *Geology* **18**, 1073-1077.

———— & WILLIAMS, P.F. (1984): Structure, origin and concentration of the Brunswick 6 and 12 orebodies. *Econ. Geol.* **79**, 1669-1692.

VERNON, R.H. (1986): Evaluation of the "quartz-eye" hypothesis. *Econ. Geol.* **81**, 1520-1527.

———— & FLOOD, R.H. (1977): "Quartz-eye"-bearing porphyroidal rocks and massive sulfide deposits – a discussion. *Econ. Geol.* **72**, 698-701.

WAHL, J.L. (1978): *Rock Geochemical Exploration at the Heath Steele and Key Anacon Deposits, New Brunswick.* Ph.D. thesis, Univ. New Brunswick, Fredericton, New Brunswick.

WENNER, D.B. & TAYLOR, H.P., JR. (1971): Temperatures of serpentinization of ultramafic rocks based on O^{18}/O^{16} fractionation between coexisting serpentine and magnetite. *Contrib. Mineral. Petrol.* **32**, 165-185.

WINCHESTER, J.A. & FLOYD, P.A. (1977): Geochemical discrimination of different magma series and their differentiation products using immobile elements. *Chem. Geol.* **20**, 325-343.

WOOD, S.A. (1990): The aqueous geochemistry of rare-earth elements and yttrium. 2. Theoretical predictions of speciation in hydrothermal solutions to 350°C at saturated water vapor pressure. *Chem. Geol.* **88**, 99-125.

———— & WILLIAMS-JONES, A.E. (1994): The aqueous geochemistry of rare-earth elements and yttrium. IV. Monazite solubility and *REE* mobility in exhalative massive sulfide-depositing environments. *Chem. Geol.* (in press).

WOODLAND, A.B. & WALTHER, J.V. (1987): Experimental determination of the solubility of the assemblage paragonite, albite, and quartz in supercritical H_2O. *Geochim. Cosmochim. Acta* **51**, 365-372.

WYNNE, P.J. & STRONG, D.F. (1984): The Strickland prospect of southwestern Newfoundland: a lithogeochemical study of metamorphosed and deformed volcanogenic massive sulfides. *Econ. Geol.* **79**, 1620-1642.